VESTFOLD UNIVERSITY COLLEGE
Faculty of Science and Engineering

IMST
INSTITUTT FOR MIKROSYSTEM TEKNOLOGI

MASTER THESIS

Force/Deflection Measurements on Micromechanical Structures

Kai Axel Hals

Horten, YEAR 2007

Submitted to the Faculty of Science and Engineering, Vestfold University College, in partial fulfilment of the requirements for the degree Master of Microsystem Technology.

Abstract

Material properties of typical MEMS materials have been widely tested. Properties of MEMS structures also depend on other factors than the material properties. A measurement system has been made to measure force/deflection on microstructures to examine some of the structural properties. This is done as a stylus measurement with a loadcell and a linear actuator. First the requirements for the measurement system were established, and the method decided. Then the system was characterized, and tested on micromechanical structures. The provided structures were the SW412 accelerometer structure from Infinion SensoNor Technologies, which is a simply supported mass accelerometer structure. Measurements done on this structure were thoroughly analyzed, and this analysis will also be valid for other simply supported mass accelerometer designs. This thesis include analysis of the force/deflection curve shape, the stylus placement accuracy, the spring constant along the mass, destructive tests, process variations and measurement with bridge signals.

This thesis has been finished under the supervision by:

Supervisor Einar Halvorsen, Associate Professor.

Supervisor Xuyuan Chen, Professor.

Table of Contents

1 Introduction/Background

Mechanical properties of different materials have been widely tested with various methods over the years. These material properties are now well known and understood. When producing MEMS-devices today the manufacturers depend heavily on the known properties of the materials they use. One would think that properties of micro structures would depend on its geometry and the properties of its material. This is not always the case. The behavior of micro structures is not always what would be expected from the known geometries and material properties. For this reason it would be useful to have a measurement setup that could measure the mechanical properties of micro structures, so that the analytic and simulated properties of the structures could be verified. In this project I have created a measurement system to measure the force and deflection on microstructures, so that some of the mechanical properties of the tested structures can be determined.

This thesis is built up in a similar order as the work performed in the project. First thing that had to be established was the requirements for the measurement system. In the start a lot of time was also used searching the literature and trying to find similar existing measurement methods. These methods were studied and some were used as inspiration when deciding on the measurement principle used in this project. A stylus measurement was chosen, with a loadcell to measure the force and a linear actuator to deflect the structures. After the parts were assembled the measurement system was characterized to find the certainty and tolerance of the measurements. Finally measurements on provided structures were performed and analyzed to test the measurement setup.

This thesis was proposed by Trond Inge Westgaard at Infinion SensoNor Technologies and he also provided the structures used to test the measurement system. These structures were the SW412 accelerometer structure. The structure consists of a mass, simply supported by one spring. Since this was the provided structures all of the extensive measurements and analysis performed in this thesis is done on this type of structures, simply supported mass. The analysis of the measurement results will therefore also be valid for other types of simply supported mass structures. However the measurement system could be used to measure force and deflection on all kinds of deflectable structures such as simply supported cantilevers, doubly clamped mass, membranes, etc. In the case of measurements on other kinds of structures the measurement results must be analyzed in a similar fashion as done with the simply supported mass in this thesis.

2 Requirements for method

Before finding a method or finding parts for a measurement setup I had to find the requirements for the system. I divided this in to force requirements, deflection requirements and requirements for the size of the stylus tip. This is discussed in the following sections.

Since this thesis was proposed by Trond Inge Westgaard at Infinion SensoNor Technologies he also provided structures to use for testing in this project. These structures were two wafers of the SW412 accelerometer structure. These structures have been thoroughly tested in the past and most of their properties are well known, therefore it is an ideal structure to use as a structure to test the measurement setup. When finding the requirements for the force/deflection measurement system the SW412 was used as a starting point, and a margin was added so that also other microstructures could be tested. The specifications of the structure was found in the datasheet for the SW412 [1], and the used values are given in Table 2-1.

Table 2-1: Specifications SW412

Length of mass	187±2 µm
Width of mass	822±2 µm
Thickness of mass	23.1±1 µm
Length of spring	63±2 µm
Width of spring	80±2 µm
Thickness of spring	3.2±0.3 µm
Excitation voltage bridge	3±1 V
Sensitivity	35±10 µV/Vg

2.1 Force

From simple calculations and Ansys simulations the expected applied force needed to reach fracture in the SW412 accelerometer structure is found.

The calculations are based information given on the first meeting at SensoNor 17.01.06 with Westgaard and Westby. It was claimed that the spring constant of the SW412 accelerometer was approximately 10 N/m, and the angle of the structure when fracture occurs was approximately 70 degrees. The following calculations in is based on the simple relationship F=kx, and simple geometric considerations of the SW412 accelerometer.

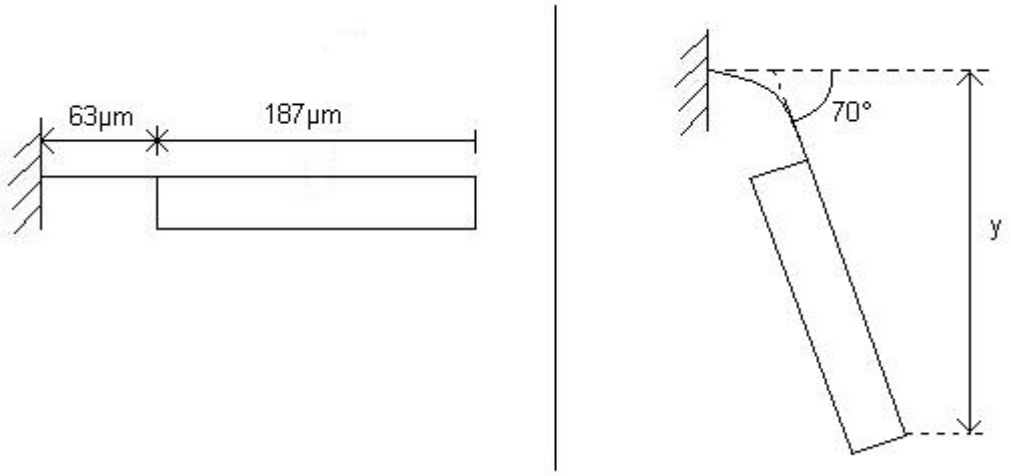

Figure 2-1: Force/deflection calculation

Deflection with 70 degrees angle at fracture:

$$y \approx 250\mu m * \sin 70° \approx \underline{235\mu m} \qquad (2.1)$$

When the deflection is 235µm and the spring constant is given to be 10 N/m, the force is found:

$$F = ky = 10N/m * 235\mu m = \underline{2.35mN} \qquad (2.2)$$

The result in Equation 2.2 gives a force of approximately 2 mN to reach fracture.

The simulation is based on a simple box model of the SW412 and the reported fracture stress of single crystal silicon found in the literature. This fracture stress varies a lot because of irregularities in the structure, e.g. sharp edges etc. Different sources give different values of the fracture stress, an estimate of 2-4 GPa seems to be a reasonable figure [2-4], but values up to 10 GPa have been registered. With the simulation the maximum stress on the structure was monitored while the applied force was stepwise increased. In Table 2-2 the results from both linear and nonlinear simulations are shown.

Table 2-2: Simulated maximum stress.

	1.5 mN	**3.0 mN**	**7.5 mN**
Linear	1.99 GPa	3.99 GPa	9.97 GPa
Nonlinear	1.88 GPa	3.58 GPa	7.12 GPa

To be sure to reach failure the maximum fracture stress of 10 GPa is used, this stress is reached with a force of 7.5 mN with linear simulations. A little more force is needed to reach this stress with the nonlinear simulations. The nonlinear simulation is probably the most accurate since with such high forces the deflections are big.

The maximum stress is also calculated with simple linear calculus using the theory of bending of beams:

$$\sigma_{\max} = \frac{h}{2}\frac{M}{I} \qquad (2.3)$$

h is the spring thickness (3.2 µm). *M* is the moment, which will be the distance from the support of the spring to where the force is applied on the mass multiplied with the applied force (156.5 µm *x). *I* is the moment of inertia (w*h^3/12) which is 218 μm^4.

$$\sigma_{\max} = 1.1486 * 10^{12} * x \quad \text{(Pa)} \qquad (2.4)$$

In Equation 2.4 x is the applied force. The maximum stress is plotted with various forces in Figure 2-2.

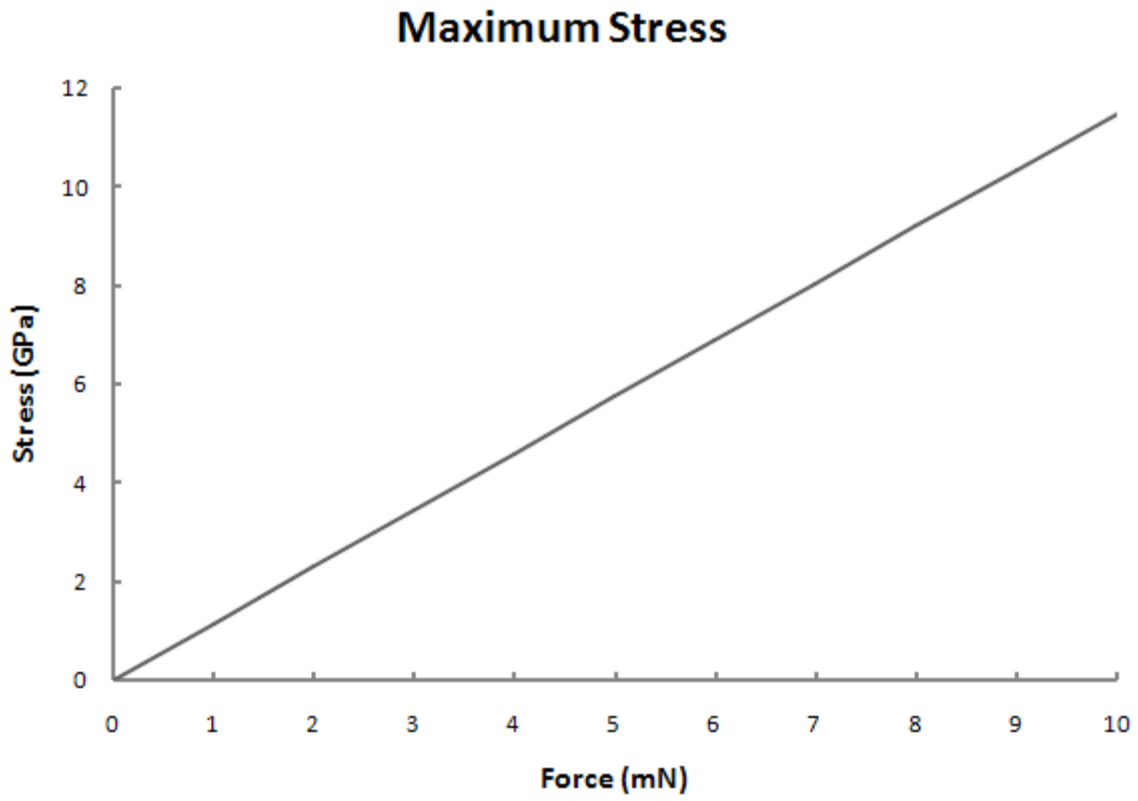

Figure 2-2: Maximum stress.

Figure 2-2 shows that a stress of 10 GPa is obtained with a force of approximately 9 mN.

With these simple calculations and simulations I set the force-range needed for the measurement system to at least 0-10 mN. This range is set with the thought of doing measurement on the SW412. If other structures are to be tested this range might need to be changed. The resolution of this force was discussed in the meeting with Westgaard, Westby, Halvorsen and Hals 17.01.06, the desired resolution of the force was 10 µN. With this force range and resolution the accuracy of the force will be 0.1 %.

2.2 Deflection

The deflection was also found in the previous calculations and simulations. Maximum deflection (at the tip of the structures) in the simulations is shown in Table 2-3.

Table 2-3: Simulated maximum deflection.

	1.5 mN	**3.0 mN**	**7.5 mN**
Linear	67 µm	133 µm	333 µm
Nonlinear	63 µm	116 µm	209 µm

The maximum deflection depends on the point chosen to load the structure (spring/mass, centre of mass, end of mass). Forces applied at the centre of mass (com) will best represent the gravity forces acting on the mass of the structure when it is in use. If the point is on the spring larger forces are needed to reach fracture, but the deflection needed to be measured will be small. On the contrary if the point is on the end of the mass smaller forces are needed, but larger deflections will be measured. By calculating the spring constant of the structure I find how rigid the structure is at different points. This was done by using theory of bending of beams:

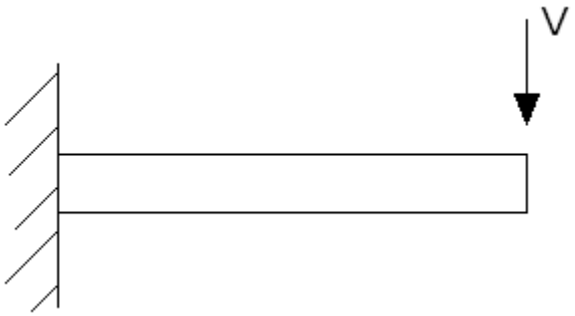

Figure 2-3: Shear force on spring

$$v = \frac{L^3}{3EI} * V \tag{2.5}$$

Since k=V/v, the spring constant k is:

$$k = \frac{3EI}{L^3} \tag{2.6}$$

Along a spring of length 63µm the spring constant is:

$$k(x) = \frac{3EI}{(L-(63-x))^3} \tag{2.7}$$

Calculation of the spring constant on the mass is a little more complicated:

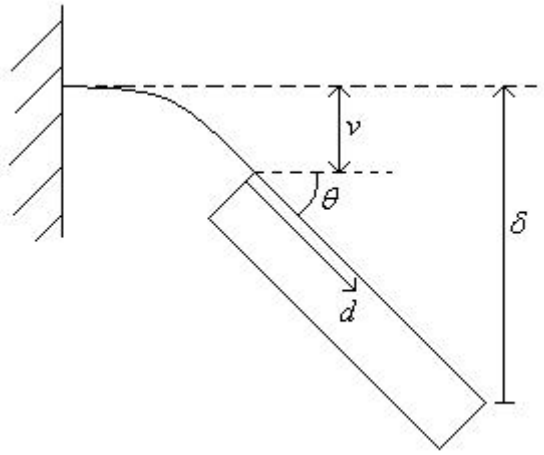

Figure 2-4: Deflection on structure.

$$\delta = v + d\tan\theta \approx v + d\theta \tag{2.8}$$

Where:

$$v = (\frac{L^3}{3EI} + \frac{L^2 d}{2EI}) * F \tag{2.9}$$

$$\theta = (\frac{L^2}{2EI} + \frac{Ld}{EI}) * F \tag{2.10}$$

Insert the Equation 2.9 and 2.10 into Equation 2.8:

$$\delta = (\frac{L^3}{3EI} + 2\frac{L^2 d}{2EI} + \frac{Ld^2}{EI}) * F \tag{2.11}$$

$$\delta = \frac{L}{3EI}(L^2 + 3Ld + 3d^2) * F \tag{2.12}$$

Since k=F/δ, the spring constant k is:

$$\underline{k(d) = \frac{3EI}{L(L^2 + 3Ld + 3d^2)}} \tag{2.13}$$

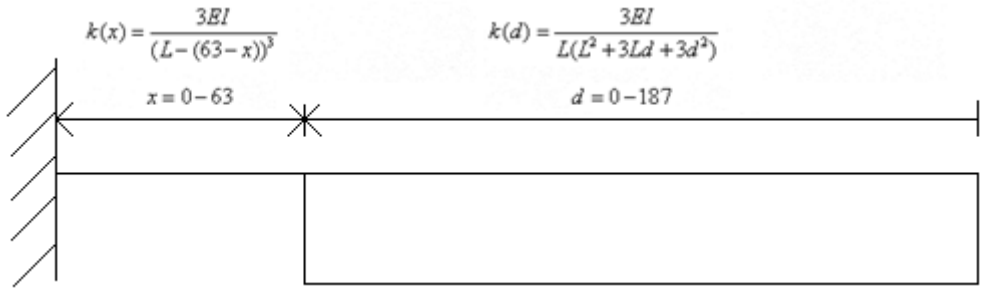

Figure 2-5: Equation for spring constant on spring and on mass.

The spring constant is then plotted in Figure 2-6 with E=170 GPa.

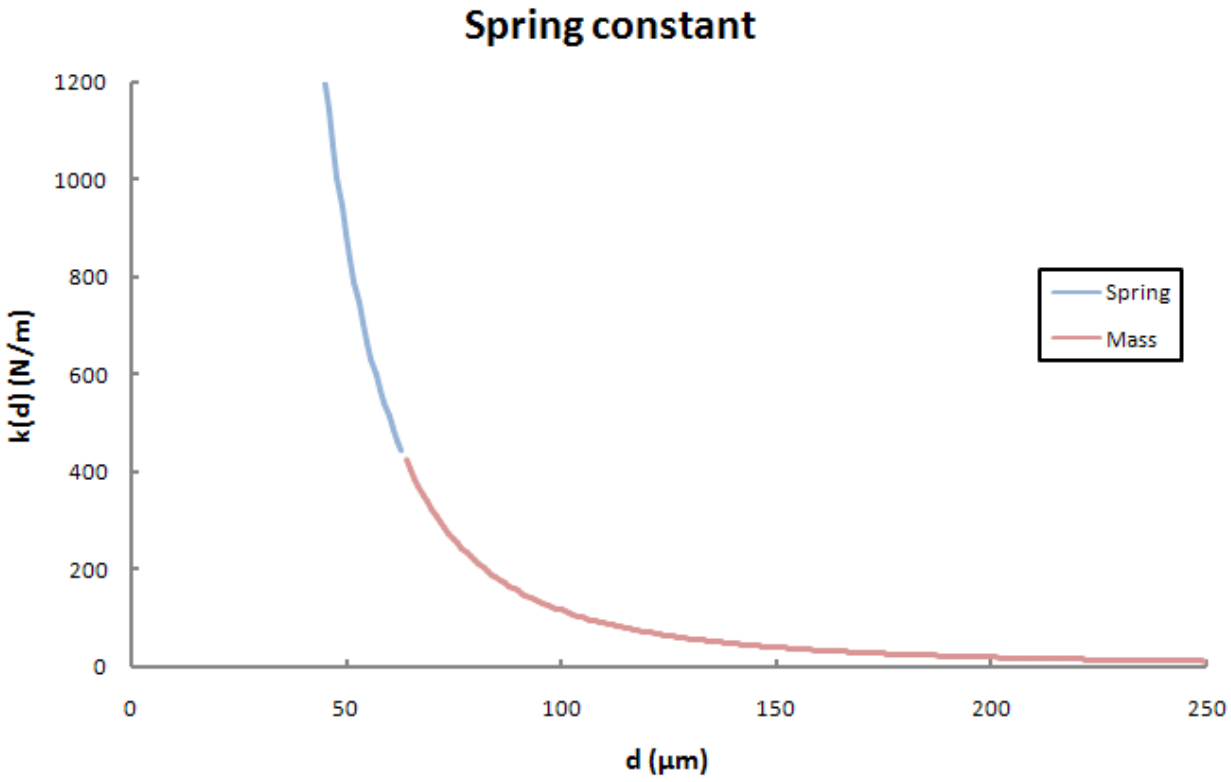

Figure 2-6: Spring constant SW412.

In Figure 2-6 it is shown that the spring constant is very high on the spring (0-63 µm) and then decreasing out on the mass. This gives that a larger force is needed for a small deflection of the structure if the force is applied on the spring. And on the mass a smaller force will be needed for the same deflection, with the tip of the mass needing the smallest force.

By plotting the deflection at a set force using the fact that F=kx (x=F/k), it is easy to see how the deflection varies with the point chosen to apply the force. In Figure 2-7 the deflection is shown with a set force of 1.5 mN used.

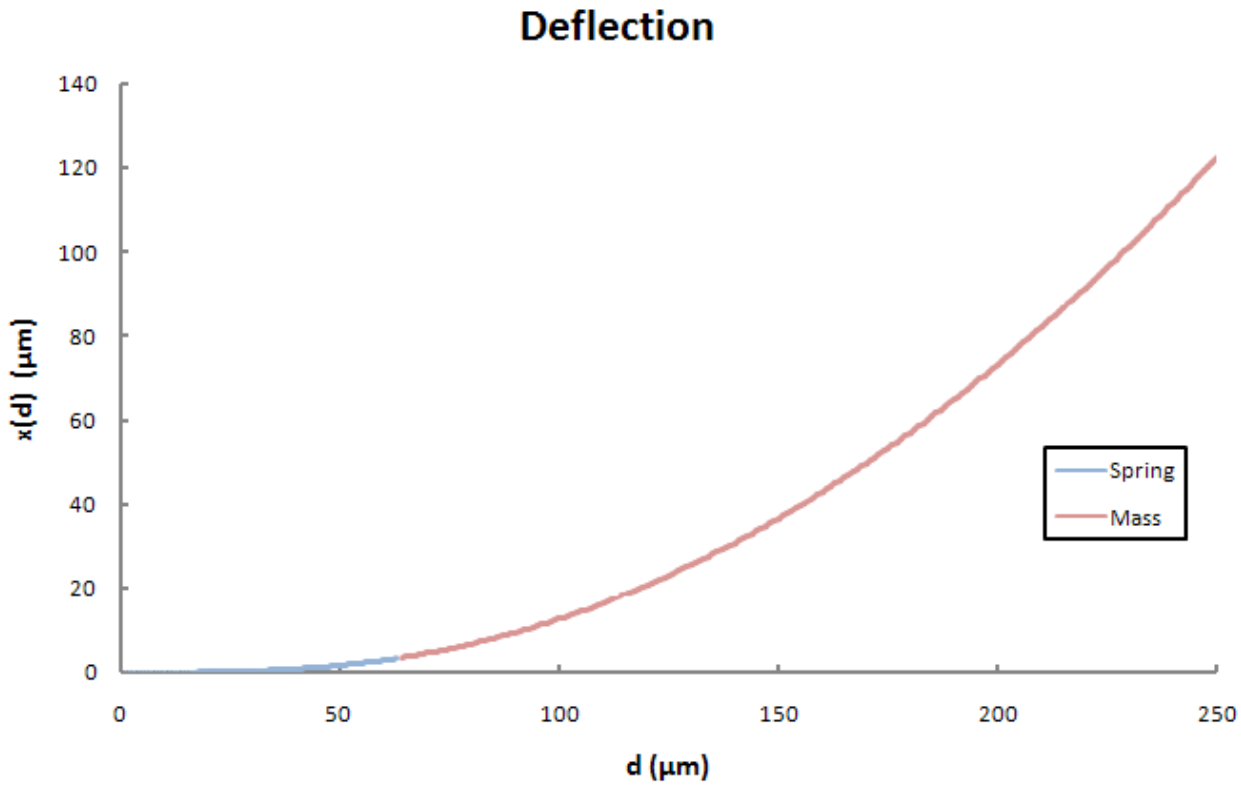

Figure 2-7: Deflection SW412 with a set force of 1.5 mN.

With these simulations, calculations and plots a deflection of a couple of hundreds µm is found to be required for the measurement system. The resolution of this deflection should be at least 0.1 µm, so that the error in the deflection measurement is small.

2.3 Stylus tip size

Another requirement is the size of the tip of the measurement stylus, or to be more precise the diameter of the tip. If this diameter is too big the influence on the measurement result will be big, because the point where the force is applied will move as the structure deflects. In the mentioned meeting at Infinion SensoNor Technologies 17.01.06 this was discussed and the agreement was that the tip diameter should be in the range of 20 µm.

It is calculated how the radius of the tip will cause deviation of the point of applied force as a structure deflects.

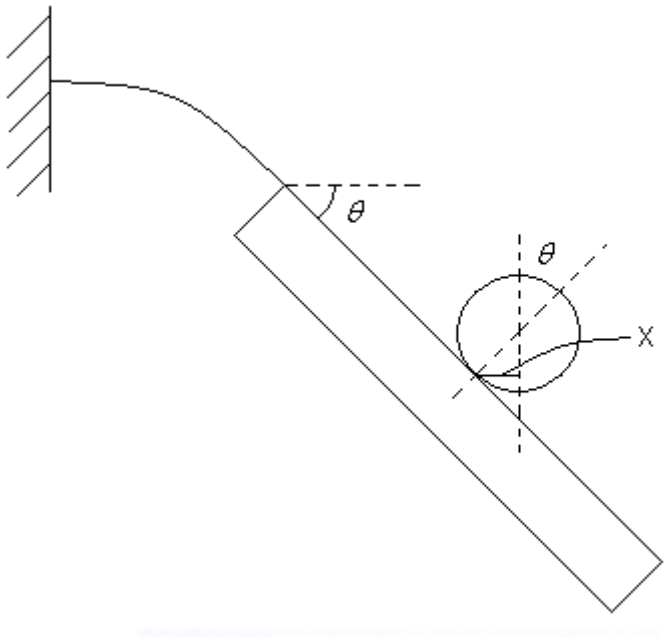

Figure 2-8: Deviation of point of applied force because of tip diameter.

From Figure 2-8:

$$x = r * \sin\theta \qquad (2.14)$$

Where *x* is the deviation, *r* is the tip radius and θ is the angle of the structure during load.

With a diameter of 20 µm the point of applied force is moved 9.4µm when the structure bends 70 degrees. This means that the arm of the force will deviate 6 % on the SW412 if the force is applied at com.

To get an idea if a stylus of this size (20 µm diameter) could withstand the magnitude of force required (0-10 mN) I have done some calculations on this with different materials and properties. The formula for maximum principal stress shown in Equation 2.15 is taken from [5], and the material properties of the different materials are taken from [6].

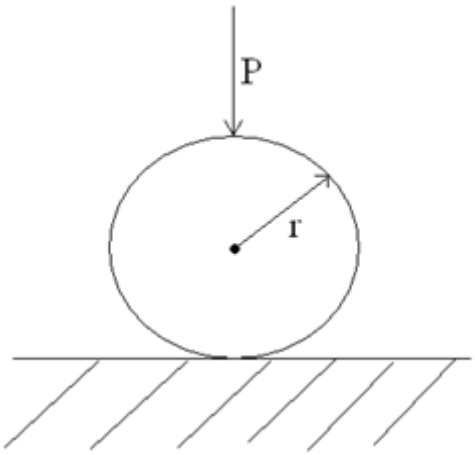

Figure 2-9: Maximum stress on stylus tip.

$$\sigma_c = 0.62\left(\frac{PE^2}{4r^2}\right)^{\frac{1}{3}} \qquad (2.15)$$

In Equation 2.15 σ_c is the maximum principal stress, *P* is the force (10 mN is used, since the force range is 0-10 mN), *E* is the modulus of elasticity and *r* is the radius of the stylus tip (10 µm). The values of *E* and the calculated values of the principal stress are shown in Table 2-4.

Table 2-4: Calculated maximum stress on tip.

Material:	**Modulus of elasticity (E):**	**Ultimate tensile strength/ Compressive yield strength:**	**Calculated max principal stress:**
High strength steel (AISI4340)	205 GPa	1448 MPa	6.3 GPa
Tungsten	400 GPa	980 MPa	9.8 GPa
Tungsten carbide	680 GPa	2683 MPa	12.46 GPa
Natural diamond	700-1200 GPa	8.6-16.5 MPa	14.3-20.5 GPa

From Table 2-4 one can see that the calculated maximum principal stress is overall higher than the ultimate tensile strength/compressive yield strength of the material. For all of the materials except diamond the values are well above. This indicates that a stylus with tip diameter 20 µm that withstand forces up to 10 mN might be difficult to find.

2.4 Summary system requirements

The wanted requirements of the measurement system are summarized in Table 2-5.

Table 2-5: Summary of measurement system requirements.

Summary measurement system requirements:	
Force	0-10 mN
Resolution	10 µN
Deflection	0-200 µm
Resolution	0.1 µm
Tip diameter	<20 µm

3 Discussion of methods

Some methods have already been proposed in the literature to do similar force/deflection measurements, e.g. testing of thin films and other microstructures. Some methods found in the literature is nanoindentation, surface profilometer, balance approach, 3D-boss-mico-probe, MFT2000. In this section these methods and other possible methods to do the desired measurement are described and discussed against the requirements.

3.1 Methods

3.1.1 Nanoindentation [7, 8]

Nanoindentation is a way to decide mechanical properties of a material, most often the hardness of the material. A force is applied to the test structure through a coil and magnet assembly or piezoelectric drives. This force thrusts a probe in to the material and leaves a “fingerprint”. This fingerprints depth can be measured by capacitive displacement sensors or the fingerprint can be studied with optics, and the material hardness can then be decided. With nanoindentation high resolutions of load and displacement can be achieved.

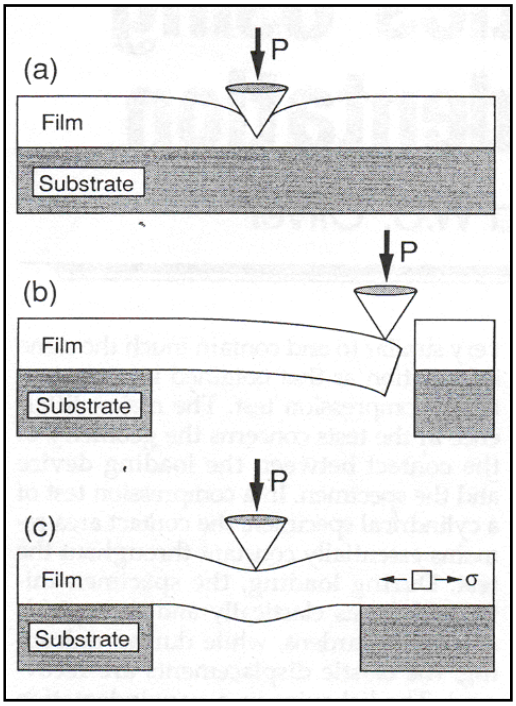

Figure 3-1: Nanoindentation principal drawing [8].

Nanoindentation has been used to do force/deflection-measurement on structures [7, 8]. The idea is to use the load applied through the probe to deflect the structures spring/mass instead of leaving a fingerprint, as shown in Figure 3-1 (b) and (c). This deflection can then be measured with the capacitive displacement sensors.

Nanoindentation test machines are found in different ranges of force and displacement. I have found a suitable test machine that meets the requirements set for the force/deflection-measurement. The problem with this method is that it is highly expensive equipment.

3.1.2 Surface profilometer [9, 10]

A surface profilometer is used to find the topography of a surface. A stylus with an applied force is scanned over the surface and the topography causes deflection of the stylus which is measured.

Surface profilometers has been used to do deflection/load-measurement on structures. The stylus is scanned along the length of the spring and mass. The stylus contacts the structure with a constant force, the structure is deflected by the stylus, and this is recorded as the instrument scans along the structure.

This data set can be analyzed in combination with the geometry of the test structure to determine material properties.

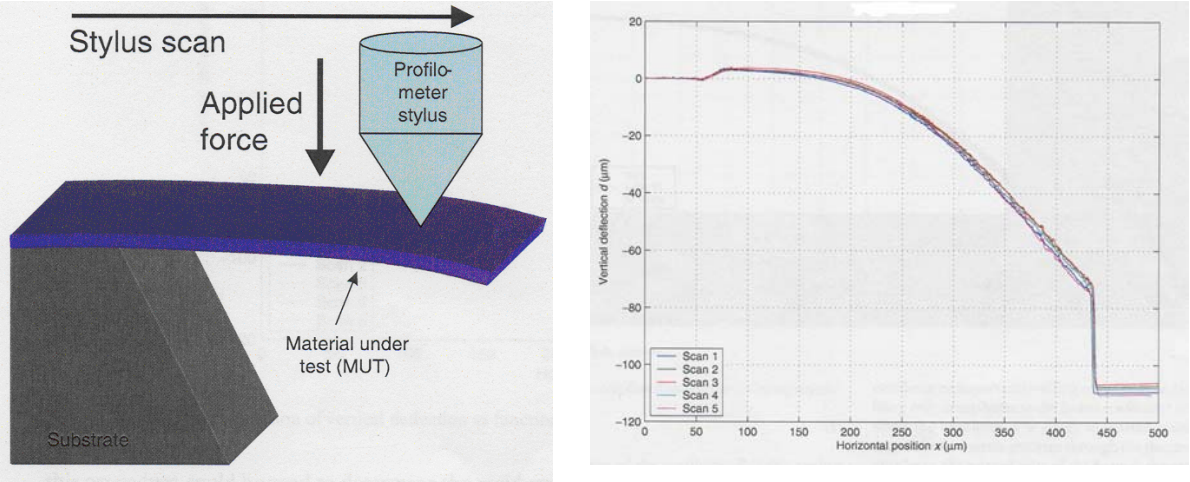

Figure 3-2: Stylus profilometer mechanical test of microstructures, principal and results [10].

In Figure 3-2 the principal of using a surface profilometer for a deflection measurement is shown, along with a curve from a deflection measurement taken from [10].

Surface profilometers are widely available laboratory test instruments. At Vestfold University College (VUC) we have a Talystep surface profilometer. I have done tests with this profilometer on a wafer with some freestanding structures. The problem with this profilometer is that it has a very limited force range and the microscope connected to it has too small magnifications so it is hard to accurately place the stylus. However I got some reasonable results from the test with the profiler, shown in Figure 3-3. The stylus was placed on a mass of a structure, the stylus was moved a short distance and then the force was increased by approximately 100 µN. This was repeated four times.

The force ranges from 0-300 µN. Each division on the plot is 0.1 µm, so the maximum measured deflection was approximately 0.12 µm. So the spring constant for this structure is calculated to 2500 N/m (300 µN/0.12 µm). Without information of the dimension of the structure or exact location of the stylus it is impossible to verify this. With this test the structure probably was far from fracture, because of the limited force range. Other more coarse profilometers are commercially available, but this is expensive equipment.

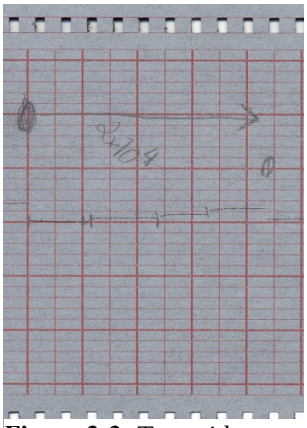

Figure 3-3: Test with VUCs surface profilometer.

An issue using this method is the force calibration. The resolution of the stylus force might be coarse, and for some profilometers the applied force is not constant as the spring deflects and the stylus is scanned in the x- or y-direction.

3.1.3 Balance approach [11]

A balance is used to measure the force and deflection. The force is applied by counterweights and the deflection is measured by an optical scale. The accelerometer is placed in one of the scale pans. A counterweight is placed in the other, to keep the balance in equilibrium. A rigid probe is adjusted to be in contact with the mass of the accelerometer without any force. Then some more counterweights are added and the pan with the accelerometer is inclined in to the probe, and a force is applied to the mass. With the optical scale reading the deflection is found.

The range of the applied force by this method fulfills the requirements of the deflection/load-measurement. Since counterweight is used to apply the load, the weight of these counterweights is the limiting factor of the force resolution. The resolution of the deflection-measurement is not given. Another drawback with this method is that the probe has to be placed on the structure manually only with help of a microscope and x- and y-micrometers.

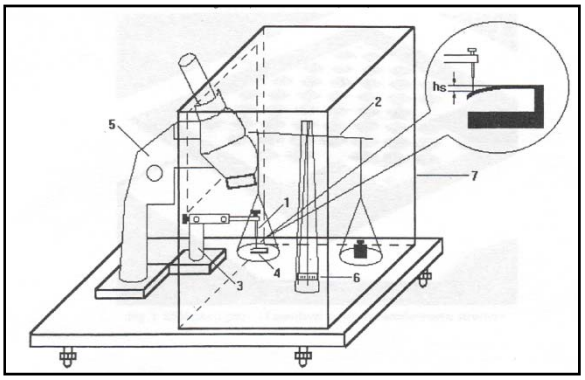

Figure 3-4: Balance approach [11].

3.1.4 MFT2000 [10, 12]

The MFT2000 is described as a specialized mechanical testing machine for micro sized specimens. The test machine is capable of applying both static and cyclic forces to microfabricated specimens.

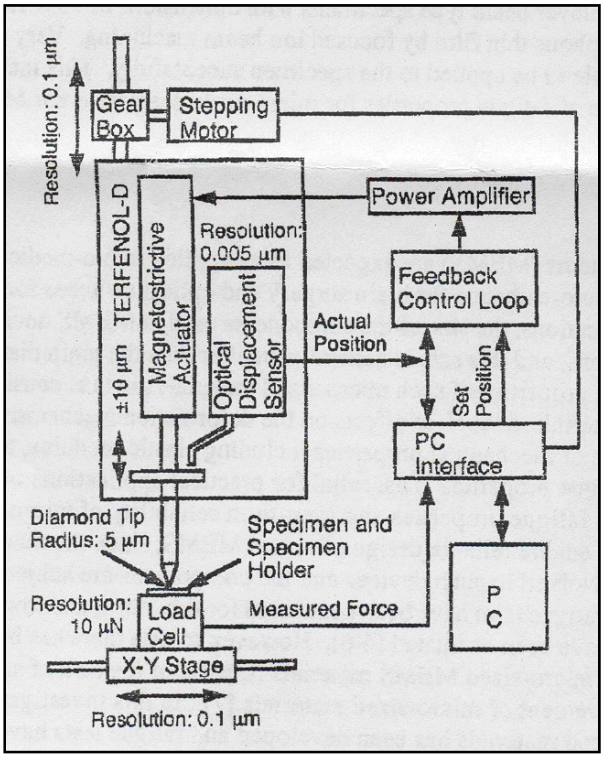

The testing equipment consists of a magnetostrictive actuator to displace the test specimen. Static force is applied to the specimen through a diamond tip with a radius of 5 µm. The magnitude of force applied to the specimen is measured by a strain gauge type load cell. The force resolution is 10 µN and the displacement resolution is 5 nm. This test machine was developed at the Tokyo Institute of Technology, and it is not a commercially available product. The principles of the test machine, shown in Figure 3-5, can however be used to build a similar test machine.

Figure 3-5: MFT 2000 [12].

3.1.5 Piezoactuator with force probe/load cell

This is a proposal to a measurement setup that has to be built from scratch. The idea is that piezoactuators displace the test structure in to a probe that measures the force the deflection yields. Piezoactuators are widely commercially available, however they give somewhat small deflections. Another challenge will be to find a suitable force probe to measure the force. AFM-tips have been explored, and also the possibility of making a probe [13] (cantilever with piezoresistive elements) .

Another solution could be to use a load cell to measure the force instead of a force probe. The principles of both methods are shown in Figure 3-6.

Force probe: **Load cell:**

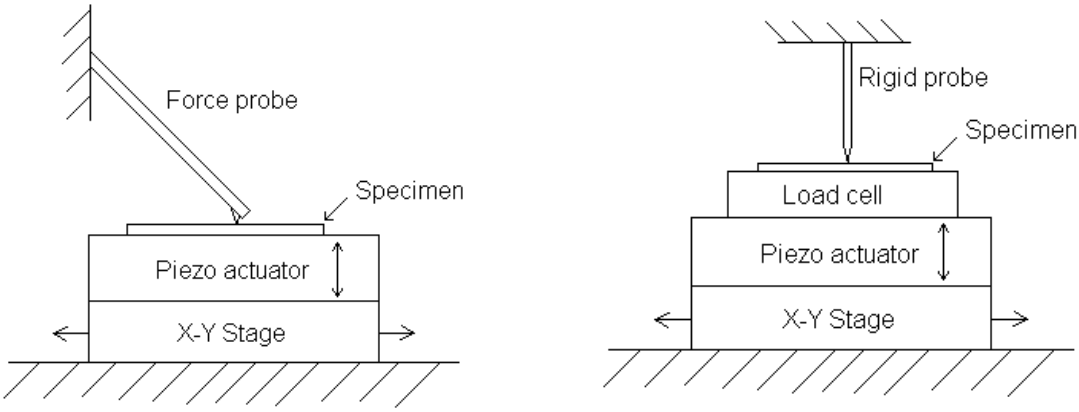

Figure 3-6: Piezoactuator with force probe/loadcell

3.1.6 Pressuresensor with stylus

In the literature I also found a method called 3D-boss-micro-probe [14]. This method is based on a silicon boss-membrane that acts as a membrane spring with a stylus in the center. On the backside of the membrane there are piezoresistive elements that detect deformations on the membrane. Deflection of the stylus during probing of a structure deforms the membrane and causes resistance changes of the piezoresistive elements.

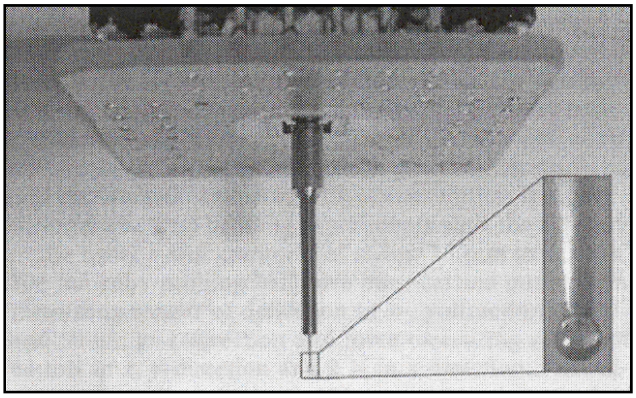

Figure 3-7: 3D Boss micro probe [14].

The stylus of the 3D-boss-micro-probe is 300 µm in diameter, and this is outside the requirements for the measurement system. The principle could however be used to build a suitable measurement system. A piezoactuator could be used to do the deflection and a stylus attached to a pressure sensor could sense the force, as shown in Figure 3-8.

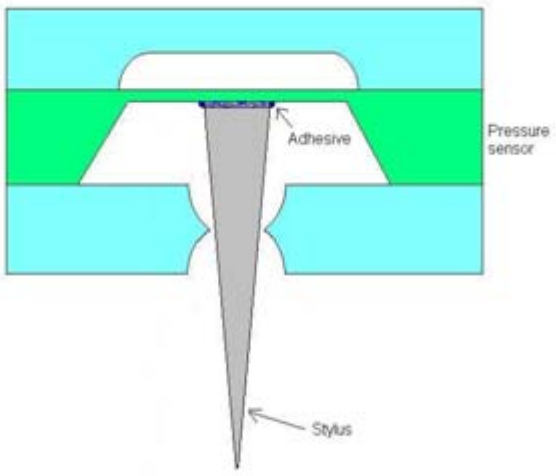

Figure 3-8: Pressure sensor with attached stylus.

3.2 Summary discussion of methods

The different specifications of the different methods are summarized in Table 3-1. Specifications that fulfill the requirements found in Chapter 2 "Requirements for method" are in green, and in red those who do not fulfill the requirements.

Table 3-1: Summary discussion of methods.

Req. / Method	**Load** 0-10 mN	**Load res.** 10 µN	**Deflection** 0-200 µm	**Defl. res.** 0.1 µm	**Tip dia.** <20 µm	**Comment**
Nano-indentation	**0-50 mN**	**1 µN**	**0-20 mm**	**0.5 nm**	**<20 µm**	Expensive
Surface profilometer	**0.5 µN-100 µN**	**?**	**0-400 µm**	**62 Å**	**5 µm**	Expensive
Balance approach	∞	**Limited by counterweights**	**?**	**?**	**<20 µm**	
MFT2000	**100 mN**	**10 µN**	**20 µm**	**5 nm**	**5 µm**	
Piezoact w. loadcell/probe	**100 mN**	**10 µN**	**0-100 µm**	**1 nm**	**<20 µm**	
Pressure sensor	?	?	0-100 µm	1 nm	<20 µm	

3.3 Deciding on method

Since this project has limited resources the methods possible to use is also limited. I got an offer on 280 000 NOK from a manufacturer on a surface profilometer that might be suitable. I say “might be” because there were difficulties getting exact figures on the load resolution. The price of nanoindentors is even higher than of surface profilometers. Since there are no suitable profilometer or nanoindentor available, these methods are not options in this project.

The balance approach is a very original method of performing these kinds of measurements. However there are uncertainties regarding the deflection measurement, and the quality of the measurement is highly dependent on manual control and readouts. For these reasons the balance approach method is rejected.

Using a pressure sensor with an attached stylus was also rejected. After contacting a specialist on adhesives the response was that the connection of the stylus to the membrane would be possible, but probably difficult. He also pointed out that the properties of the adhesive joint would be hard to predict, and that it most probably also would change the properties of the membrane in the pressure sensor. In addition a suitable stylus would probably have to be custom made.

The MFT2000 is not a commercial available product, but the principal of using an actuator to do the deflections and a loadcell to measure the load can be used to build a measurement system, as suggested in Chapter 3.1.5 “Piezoactuator with force probe/loadcell”. The challenge will be to find the parts to meet the requirements, and then assembling the different parts. A suitable loadcell, actuator and stylus must be found. An actuator to meet these requirements is not that hard to get a hold of. However a loadcell and stylus which meets the requirements are not standard equipment. The parts found and used in the measurement setup are described next in Chapter 4: “Measurement setup description”.

4 Measurement setup description

After the method to do the measurement was decided, there was a search for suitable parts for the setup. In Chapter 4.1 “Setup” the measurement setup is described, in Chapter 4.2 “Hardware” the specifications and description of the individual parts are given and in Chapter 4.3 “Software” the software of the measurement system is described.

4.1 Setup

The measurement system consists of a Loadcell, a Z-actuator, a stylus, an AD-converter and an X-Y-table. A principal drawing of the setup is shown in Figure 4-1.

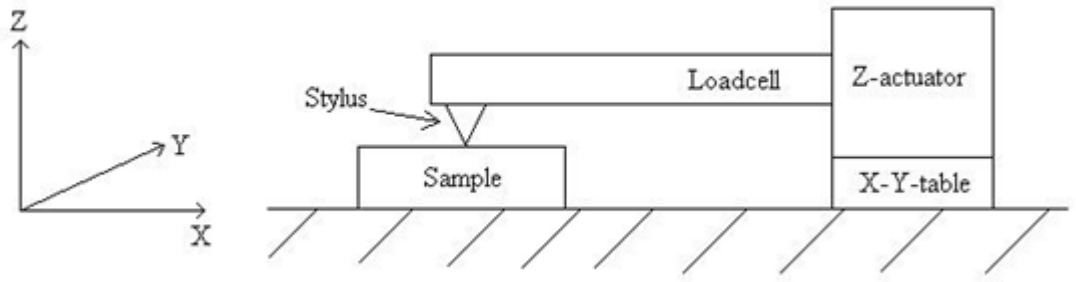

Figure 4-1: Principal drawing measurement setup.

The Z-actuator deflects the structures and the loadcell measures the force. The Z-actuator is controlled by a computer through Labview software. The loadcell is connected to an AD-converter which is connected to a computer and with Labview software the force is obtained from the loadcell.

In Figures 4-2 – 4-4 pictures of the measurement setup are shown.

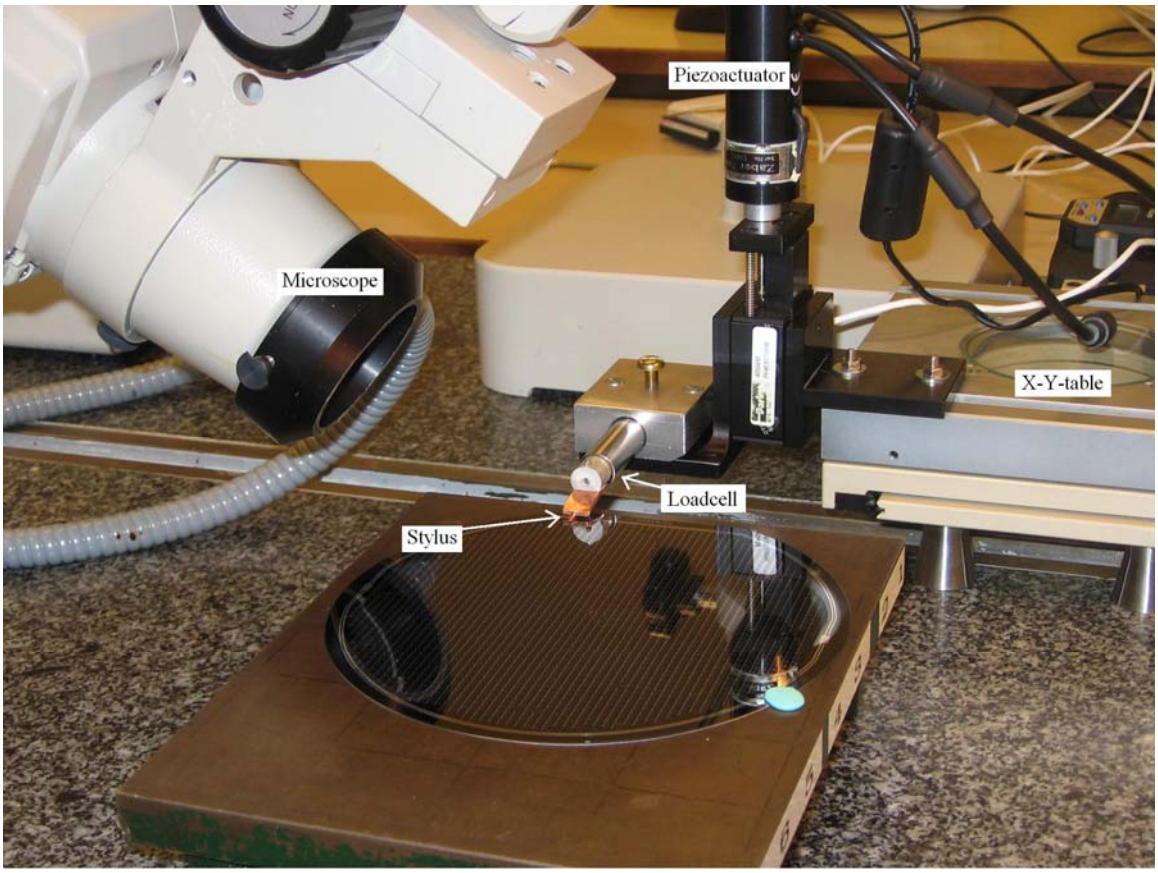

Figure 4-2: Measurement setup.

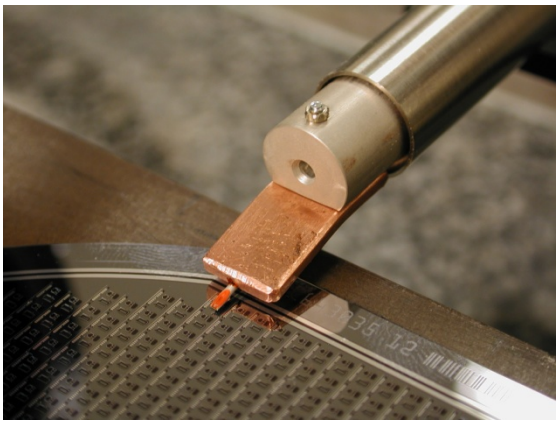

Figure 4-3: Loadcell with stylus.

Figure 4-4: Stylus.

The stylus is attached to the loadcell through a connection shown in Figure 4-3. The stylus is attached to the connection with adhesive, and the connection is attached to the loadcell with a screw and a nut. The loadcell was then connected to a translation stage which the Z-actuator can actuate in the Z-direction. This whole system was then put on an X-Y-table.

4.2 Hardware

Loadcell

The loadcell is a Honeywell 25g MBL Minigram beam loadcell. The loadcell was ordered from "Elektronisk Måleteknikk AS". Key specifications given from manufacturer:

Load range:	0-25 grams
Non-Linearity and Hysteresis (max):	±0.1% F.S.
Non-Repeatability (max):	±0.03% F.S.
Output:	20mV/V
Resolution:	Infinite (!)

Actuator

The Z-actuator is a Zaber CE Linear actuator, 28 mm, ordered from Edmund Optics. This actuator was also ordered with some translation stages and brackets. Key specifications given from manufacturer:

Travel range:	28 mm
Resolution:	0.1 µm
Repeatability:	±0.3 µm (typical)

Stylus

The stylus is a cartridge stylus from Shure, model SS35C-Q. Ordered from www.kabuse.com. Key specifications given from manufacturer:

Tracking force:	4-5 grams
Tip radius:	17.78 µm (0.7 mil)

AD-converter

To handle the signal from the loadcell on a computer, I use an AD-converter. I used one already available in VUC. This is a Texas Instruments USB 6009 AD-converter. Key specifications given from manufacturer:

Analog input resolution:	14 bits
Max analog input sample rate:	48 kS/s

X-Y-table

I use an X-Y-table already available on VUC. This is a table with manual controls and digital display of the movement. The resolution of the movement on the digital display is 1 µm.

Microscope

I use available microscopes from Infinion SensoNor Technologies and VUC. These are laboratory microscopes which can view structures from different angles. Magnification is up to 90x.

4.3 Software

To control the actuator and readout results from the loadcell, I use Labview. To control the Z-actuator I use a demo program for Labview provided from the supplier of the actuator. To get the signal from the loadcell it is connected to an AD-converter. The signal from the AD-converter is processed in Labview through a DAQ-assistant. The frontpanel of my Labview-program is shown in Figure 4-5.

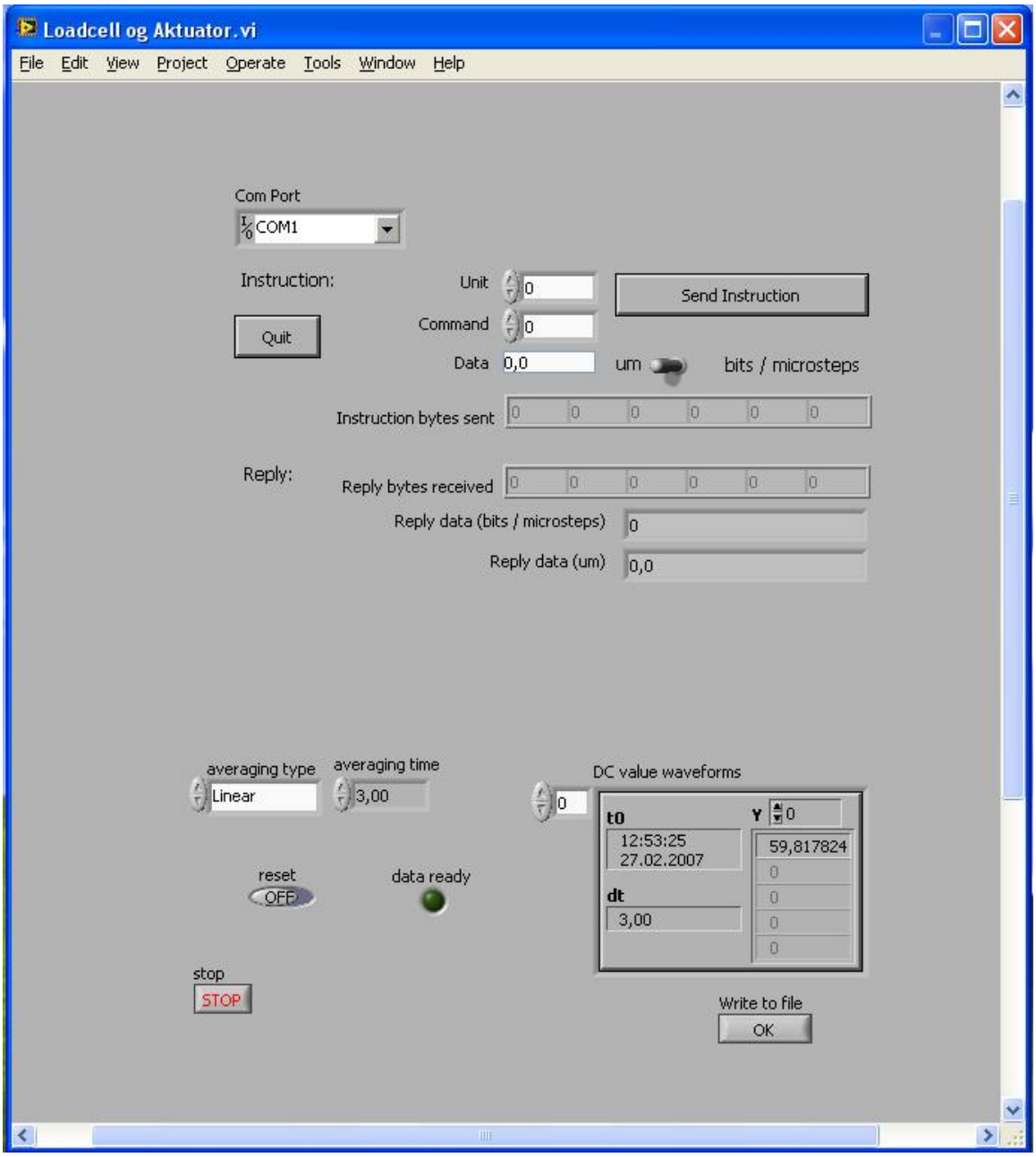

Figure 4-5: Frontpanel LabView.

The upper part of the frontpanel is where the actuator is controlled. Different commands can be sent such as absolute and relative position, home, return position, etc. The lower part is the readout from the loadcell. Here the averaging time can be controlled and the force is read out. The sample rate of the signal is controlled in the DAQ-assistant. By pressing the “Write to file” button the force readouts are written to a text file. The block diagram for the loadcell part is shown in Figure 4-6.

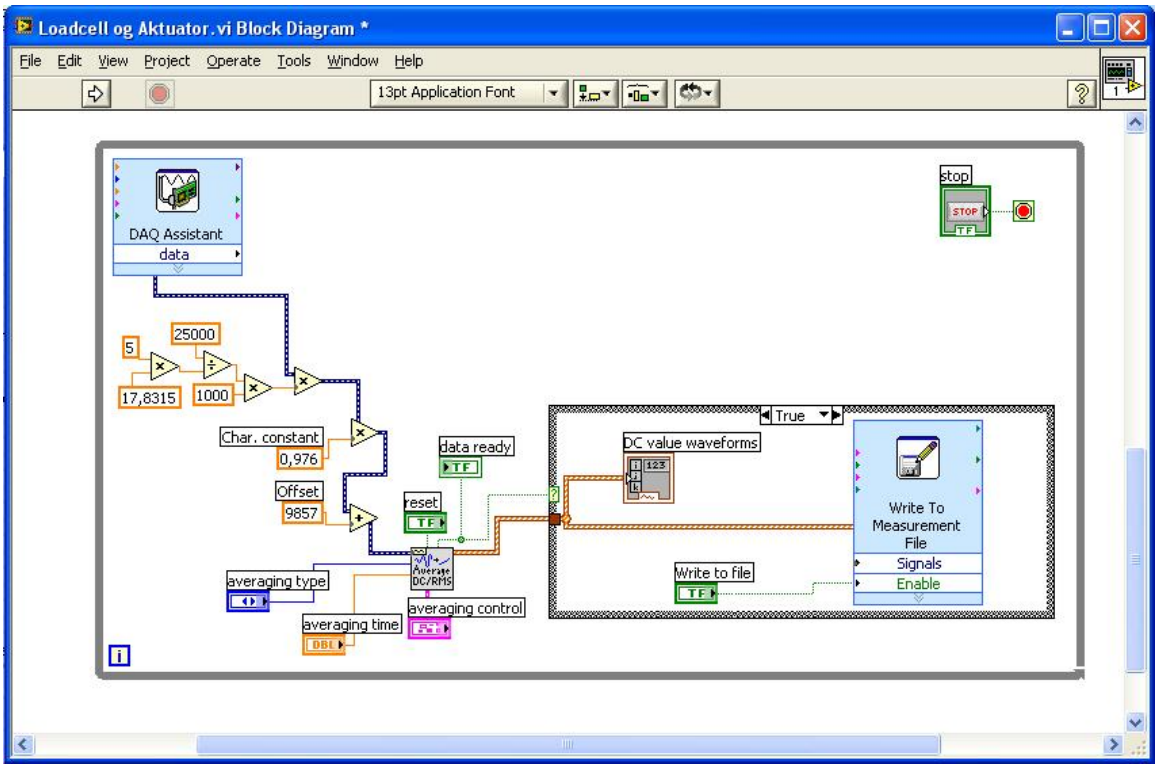

Figure 4-6: Block Diagram LabView.

In the block diagram in Figure 4-6 the signal from the DAQ-asistant is multiplied with the calibration specifications provided from the supplier of the loadcell. In addition it is multiplied with a characterization constant from Chapter 6.4 “Calibration with microprecision scale”. Then the offset is corrected before the signal is averaged and the readouts can be written to a text file. From this text file the results are loaded in to Excel and the measurement data are presented in plots as shown in Figure 5-1 on the next page. (All Excel files used to make these plots are enclosed in the CD-rom provided with this thesis.)

5 Initial measurement

After all the parts of the measurement system were connected as described previously in Chapter 4 “Measurement setup description”, I ran an initial test measurement on the SW412 accelerometer structure. In this measurement the stylus was placed as close to the centre of the mass as possible using a microscope, as shown in Figure 5-2. I deflected the mass in increments of 10 µm and measured the force at each increment. The result is shown in Figure 5-1.

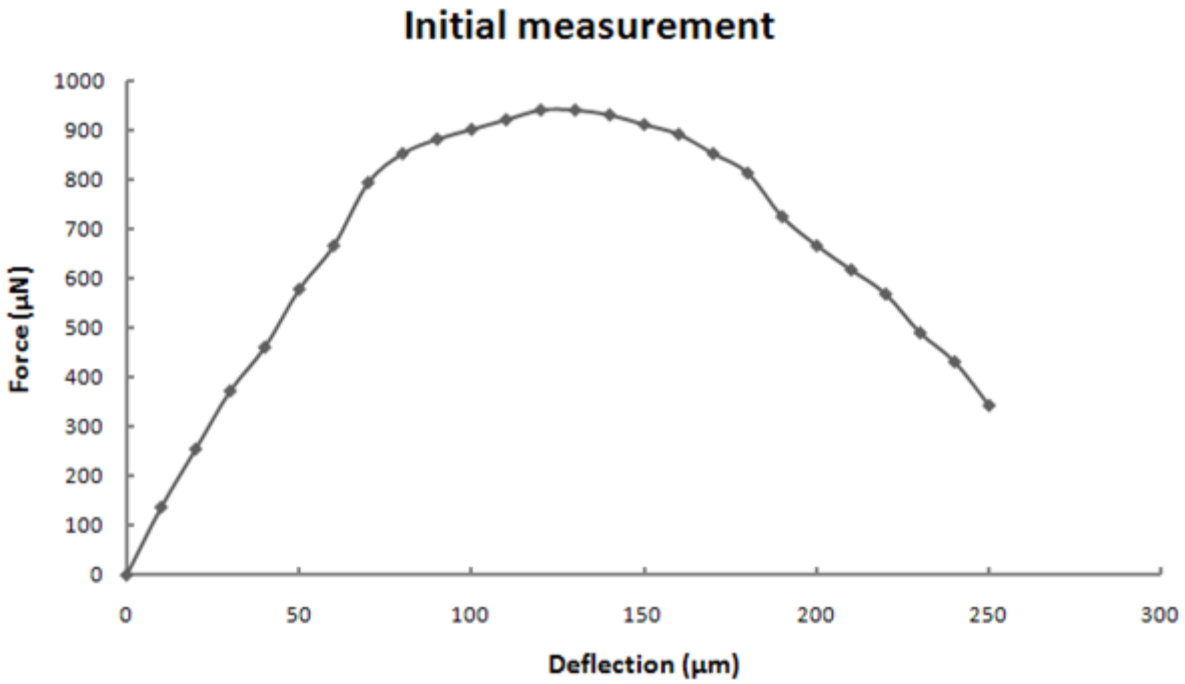

Figure 5-1: Initial force/deflection measurement.

In Figure 5-1 the relationship between the applied deflection and the measured force is shown. The deflection is along the x-axis of the curve and is given in µm, and the measured force in µN is on the y-axis. As seen in the figure there is a somewhat linear relationship between the force and the deflection at small deflections (approximately 0-70µm). After this the curve is no longer linear. The reason for this is the geometry of the structure, it is a simply supported mass. An in-depth analysis of the shape of the force/deflection curve for simply supported mass structures is done in Chapter 7.2 “Analysis of the force/deflection curve shape”. This initial measurement was performed before the measurement setup was characterized and settings optimized as explained in Chapter 6 “Characterization measurement setup”. Because of this the curve is somewhat uneven.

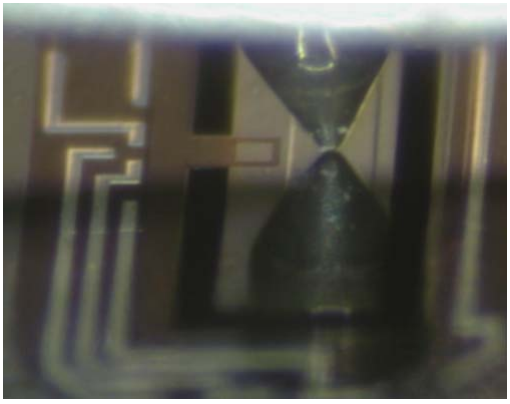

Figure 5-2: Stylus placed at com.

6 Characterization measurement setup

In Chapter 4.2 “Hardware” the specifications from the manufacturers of the different parts of the measurement setup was presented. In this chapter the specifications of the whole measurement setup will be evaluated.

6.1 Signal from loadcell

The signal from the loadcell is studied in a Labview program. As seen in Figure 6-1 the signal has noise added to it. From studies of the power spectrum density of the signal (Figure 6-2) there are no dominant frequencies, so this is white noise.

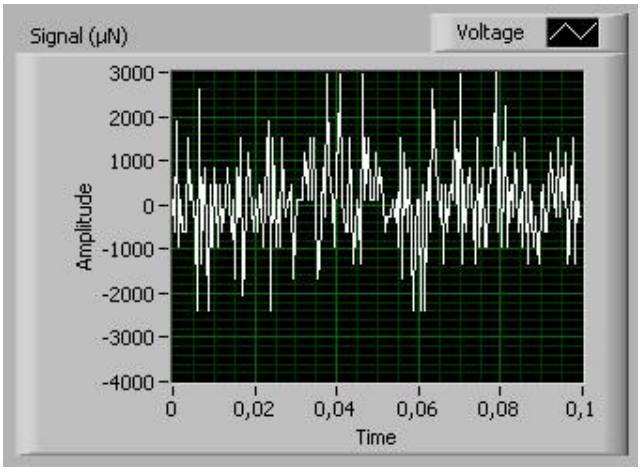

Figure 6-1: Signal loadcell.

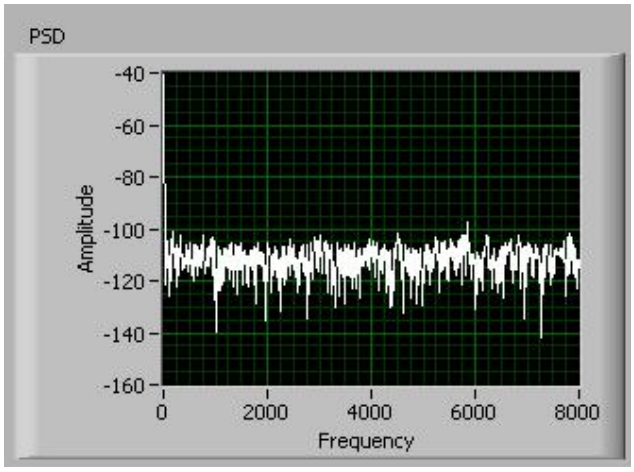

Figure 6-2: Power spectrum density loadcell signal.

The standard deviation in the signal from the loadcell is found with Labview to be 1080 µN for each single sample. To filter out this noise the signal is averaged over many samples, as shown in Equation 6.1.

$$\sigma_N = \frac{\sigma}{\sqrt{N}} = \frac{1080\mu N}{\sqrt{10000}} = 10.8\mu N \qquad (6.1)$$

In Equation 6.1 σ is the standard deviation, σ_N is the standard deviation with N samples, and N is number of samples. So by averaging over 10000 samples the standard deviation of the measurement is 10.8 µN. Averaging over 10000 samples can be obtained by using a 2000 Hz sample rate from the AD-converter and averaging over 5 seconds.

To verify this standard deviation I have done some measurements on one of the provided structures. I have done thirty measurements in a series with identical deflection at the centre of mass, so the force readouts are also expected to be identical. I did one measurement series with 50 µm deflections and one with 100 µm deflections. For thirty measurements done with a deflection of 50 µm the standard deviation was 10.3 µN, and with deflection of 100 µm it was 9.5 µN.

To get the most exact measurement N has to be as large as possible. It is limited by the sample rate of the AD-converter and the averaged time. The maximum sample rate with the Ad-converter is 48kHz over all channels. I will eventually be using two channels so I choose to use a 20kHz sample rate from the AD-converter. To make the measurement somewhat time effective I use an averaging time of 3 seconds. This gives N=60000, and from the Equation 6.1 the standard deviation will then be 4.4 µN. This is verified with another thirty measurements with the same deflection. The standard deviation from this measurement was 6.8 µN. These values are close to the wanted resolution of 10 µN from Chapter 2 "Requirements for method".

6.2 Actuator precision

The resolution of the actuator is given from the manufacturer to be 0.1µm. However the precision of the actuator is somewhat cyclic as shown in Figure 6-3, which is a graph provided from the manufacturer. This error comes from the motors used in the actuator. There are 48 poles on the motor and there is some error in their alignment. Some poles are closer together and some are further apart. That combined with the translation of the rotary motion causes the error.

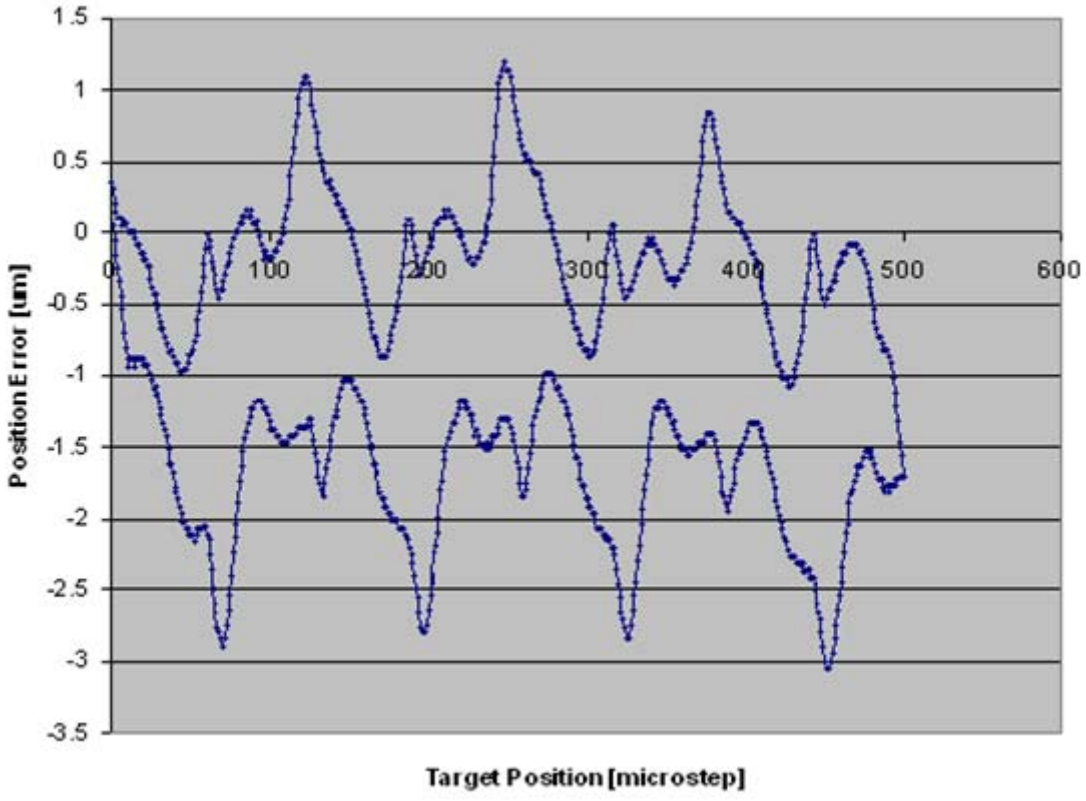

Figure 6-3: Cyclic error actuator [provided by Jesse Schuhlein at Zaber Technologies Inc.].

Figure 6-3 shows an error pattern which repeat itself every 12.7 µm (1 microstep = 0.1 µm). This error causes an error of +/-1 µm of the deflection in the measurement system. When performing measurements on structures on the centre of the mass the deflection reaches a few hundred µm before

fracture. With these deflections this error is negligible small. However when doing measurements close to the spring or in the linear area the deflections are smaller and this has to be taken in to consideration. One way of canceling out this error would be to do the measurements with deflection in increments of X*12.7µm (X=1, 2, 3,….), this way the measurements would be done at the same place on the error graph, and the error would cancel out.

In Figure 6-4 a measurement is done in the linear area of the curve with no consideration of the microstep error. The measurement was done with stepsize 3.2 µm (12.7µm/4) on the deflection. As seen in the figure there is a repeatable pattern. What should be measured is the linear curve, but because of the microstep error the measured curve deviates from this curve.

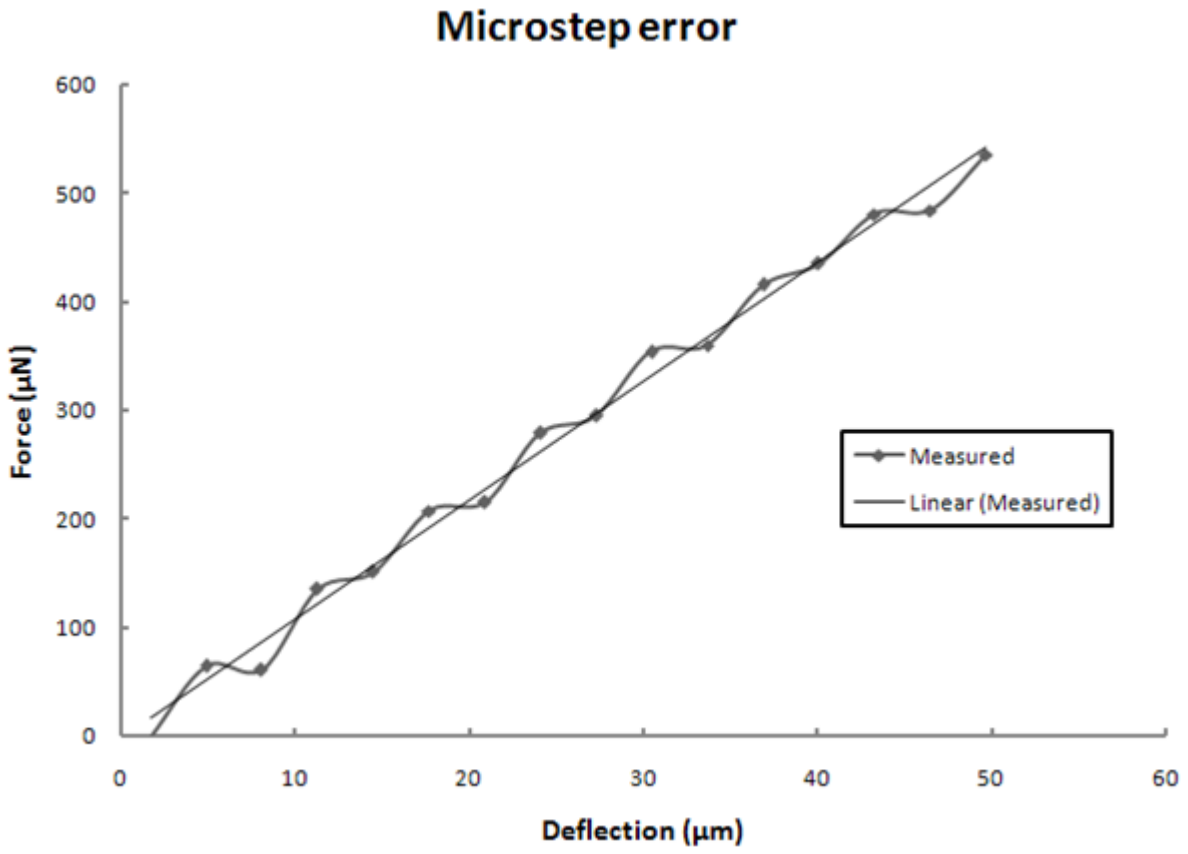

Figure 6-4: Microstep error.

6.3 Accuracy of stylus placement

How accurately the stylus can be placed on the mass in the X- and Y-direction depends on the magnification of the microscope used and the accuracy of the X-Y-table. The exact accuracy of the placement of the stylus is therefore difficult to establish. It will also be different from structure to structure. On some structures one might have some reference point to aim for when placing the stylus such as a corner, an edge, a spring, a metal conductor, etc. How close the stylus is placed to these reference points will affect the accuracy. When using reference points it is important that the microscope and X-Y-table is perfectly aligned or else the stylus placement accuracy will be influenced.

Some structures will not have an immediate reference point and the stylus must be place on the middle of a surface or a mass. In measurements on such structures with the current microscope and x-y-table I would estimate the accuracy of placement of the stylus to be no more than ±5 μm, probably less. This might be reasonable for some structures, and too much on other structures. The stylus placement accuracy and the effects of this accuracy must be analyzed for the different structures tested with the measurement setup. (In Chapter 7.1 “Stylus placement accuracy simply supported mass” the effects of a simply supported structure is discussed.)

6.4 Calibration with Microprecision scale

To calibrate the loadcell the stylus was placed on the pan of a high precision scale with a resolution of 0.1 mg. 0.1 mg is equal to 0.98 µN (N=kgm/s^2). I did a series of measurements with deflections in intervals of 0.1 µm. Then I compared the readouts from the scale and the loadcell. The setup is shown in Figure 6-5, and the results are shown in Table 6-2.

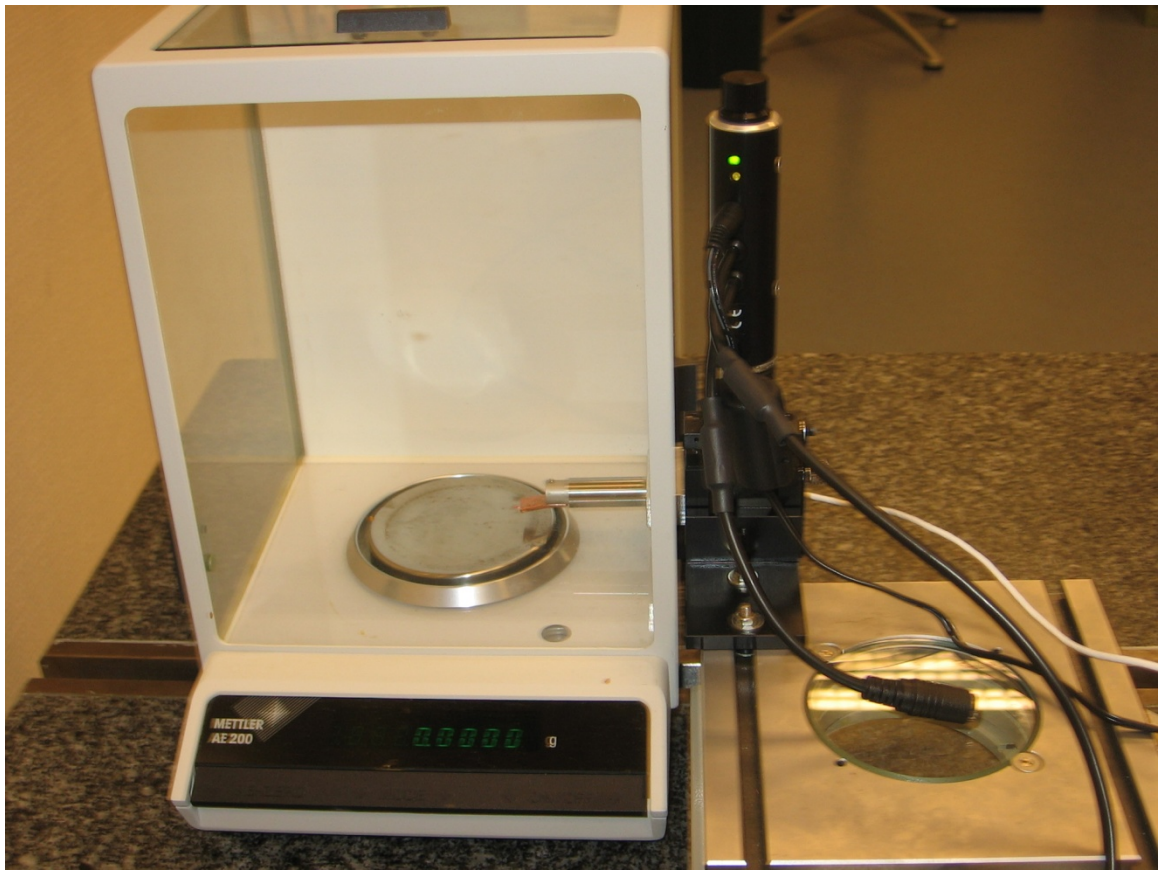

Figure 6-5: Calibration with microprecision scale.

Table 6-1: Calibration with microprecision scale.

Position (abs):	Position (rel) (µm):	Scale (mg):	Loadcell (mg):	Error (mg):	Error (%):	Characterization constant:	Springconstant (mg/µm)	Springconstant (N/m):
5920.1	0	0	0	0	0	0	0	0
5920.2	0.1	73	76	3	4.109589041	0.960526316	760	7448
5920.3	0.2	119	121	2	1.680672269	0.983471074	605	5929
5920.4	0.3	163	166	3	1.840490798	0.981927711	553.3333333	5422.666667
5920.5	0.4	195	198	3	1.538461538	0.984848485	495	4851
5920.6	0.5	240	246	6	2.5	0.975609756	492	4821.6
5920.7	0.6	265	270	5	1.886792453	0.981481481	450	4410
5920.8	0.7	323	332	9	2.786377709	0.972891566	474.2857143	4648
5920.9	0.8	374	382	8	2.139037433	0.979057592	477.5	4679.5
5921	0.9	431	443	12	2.784222738	0.972911964	492.2222222	4823.777778
5921.1	1	494	507	13	2.631578947	0.974358974	507	4968.6
5921.2	1.1	544	557	13	2.389705882	0.976660682	506.3636364	4962.363636
5921.3	1.2	602	614	12	1.993355482	0.980456026	511.6666667	5014.333333
5921.4	1.3	692	708	16	2.312138728	0.97740113	544.6153846	5337.230769
5921.5	1.4	713	731	18	2.52454418	0.975376197	522.1428571	5117
5921.6	1.5	737	754	17	2.306648575	0.977453581	502.6666667	4926.133333
5921.7	1.6	757	775	18	2.377807133	0.976774194	484.375	4746.875
5921.8	1.7	776	794	18	2.319587629	0.977329975	467.0588235	4577.176471
5921.9	1.8	818	840	22	2.689486553	0.973809524	466.6666667	4573.333333
5922	1.9	843	863	20	2.372479241	0.976825029	454.2105263	4451.263158
5922.1	2	858	879	21	2.447552448	0.976109215	439.5	4307.1
5922.2	2.1	874	897	23	2.631578947	0.974358974	427.1428571	4186
5922.3	2.2	887	909	22	2.480270575	0.97579758	413.1818182	4049.181818
5922.4	2.3	913	934	21	2.300109529	0.97751606	406.0869565	3979.652174
5922.5	2.4	930	954	24	2.580645161	0.974842767	397.5	3895.5
5922.6	2.5	956	982	26	2.719665272	0.973523422	392.8	3849.44
5922.7	2.6	972	996	24	2.469135802	0.975903614	383.0769231	3754.153846
5922.8	2.7	984	1009	25	2.540650407	0.975222993	373.7037037	3662.296296
5922.9	2.8	990	1015	25	2.525252525	0.975369458	362.5	3552.5
5923	2.9	1011	1035	24	2.37388724	0.976811594	356.8965517	3497.586207
					Avg:	Avg:	Avg:	Avg:
					2.42247325	0.976366446	473.0515968	4635.905649

As seen in Table 6-1 the readouts from the loadcell is overall slightly higher than the readouts from the scale. The reason for this is the extended arm of the stylus connected to the loadcell, shown in Figure 4-3. The loadcell is calibrated from the manufacturer in a hole on the loadcell. When the stylus is attached to this hole it adds an extra arm. This extra arm adds an extra moment to the measurements performed by the loadcell, hence the slightly higher values from the loadcell than the scale. The average characterization constant is 0.976, so the readout from the loadcell must be multiplied with this constant to obtain correct values. This is done in the Labview program discussed in Chapter 4.3 “Software”.

The high precision scale works by a force-restoration-principle, which gives that the scalepan will not deflect. By assuming that all deflections are taken up by the measurement system I can calculate the spring constant of the system. As seen in Table 6-1 the average spring constant for the system calculated by this measurement is 4635 N/m. This spring constant is orders higher than the spring constant on the mass of the structures shown in Figure 2-6. This is a good thing for the measurement because most of the deflections will be done on the structures and not on the measurement setup.

6.5 Specifications vs. requirements

In Chapter 2 “Requirements for method” the requirements for the force/deflection measurement system was established, they were summarized in Table 2-4.

Table 2-4: Summary of measurement system requirements.

Summary measurement system requirements:	
Force	0-10 mN
Resolution	10 µN
Deflection	0-200 µm
Resolution	0.1 µm
Tip diameter	<20 µm

The force specifications of the measurements setup fulfill the requirements. The loadcell has a range of 0-250 mN (0-25 grams) and standard deviation in each force measurement of 6.8 µN.

The Z-actuator can travel 28 mm and has a resolution of 0.1 µm and is inside the requirements. There is however a microstep error commented in Chapter 6.2 “Microstep error” that must be taken into account.

The stylus used has a radius of 17.78 µm which gives a diameter of 35.5 µm which is larger than the set diameter. This stylus was however the stylus found with the smallest tip diameter that could withstand the expected forces and was commercially available. Therefore this stylus was used even though it has a somewhat bigger diameter than the decided requirements. The effect of the somewhat bigger diameter will depend on what kind of structures that is tested with the measurement system.

7 Measurements on micromechanical structures with analysis

The provided structures from Infinion SensoNor Technologies were the SW412 accelerometer structure. This accelerometer structure consists of a simply supported mass. All analysis in this part of the thesis is therefore done on simply supported mass structures, and is valid for similar structures. If measurements with the force/deflection measurement system are performed on other types of structures, such as simply supported cantilevers, doubly clamped mass, membranes, etc. , these measurements must be analyzed in a similar fashion as done in this chapter for the simply supported mass structures.

Information on the provided structures for testing was given in Table 2-1, found in the datasheet of the SW412 [1]. If not other is mentioned the measurements performed in this chapter is done on the SW412 accelerometer structure.

The structures were provided on wafers. The structures on the wafers was numbered with letters (A,B,C,…) on the rows and numbers (1,2,3,…) on the columns. This was done to be able to sort out which measurements were performed on which structure.

7.1 Stylus placement accuracy simply supported mass

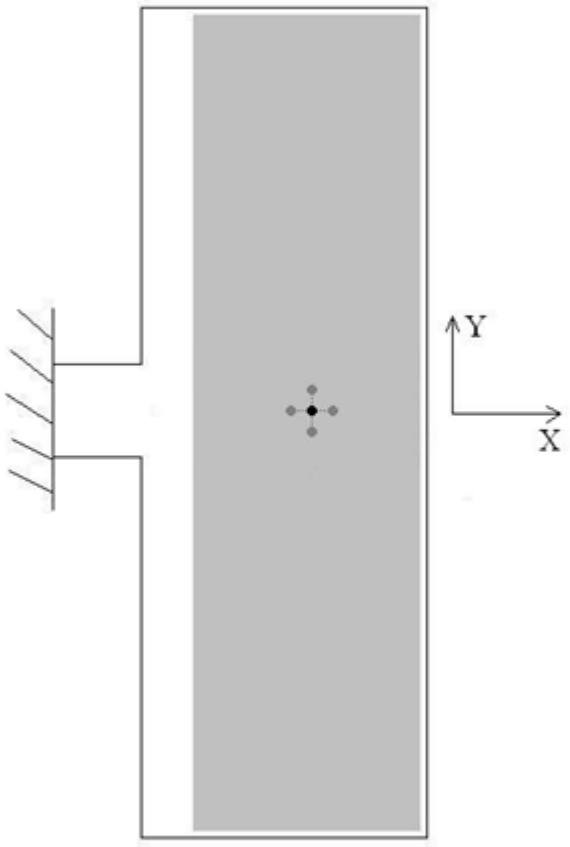

As commented in Chapter 6.3 “Accuracy of stylus placement” the stylus placement accuracy and its effect on the measurement must be evaluated for different types of structures. In this subchapter the effects will be evaluated for the SW412 structures.

The stylus has to be positioned on the mass with the help of a microscope. I have studied the effect on the result of the measurement of a small difference in the placement of the stylus. I have used the centre of mass as a starting point and then slightly moved the stylus in the x- and y-direction. This is shown in Figure 7-1.

Figure 7-1: Stylus placement.

7.1.1 Y-direction

In the y-directionin Figure 7-1 I have done 5 different measurements. One at centre of mass, zero, and then four at -20, -10, +10 and +20. The results are shown in Figure 7-2.

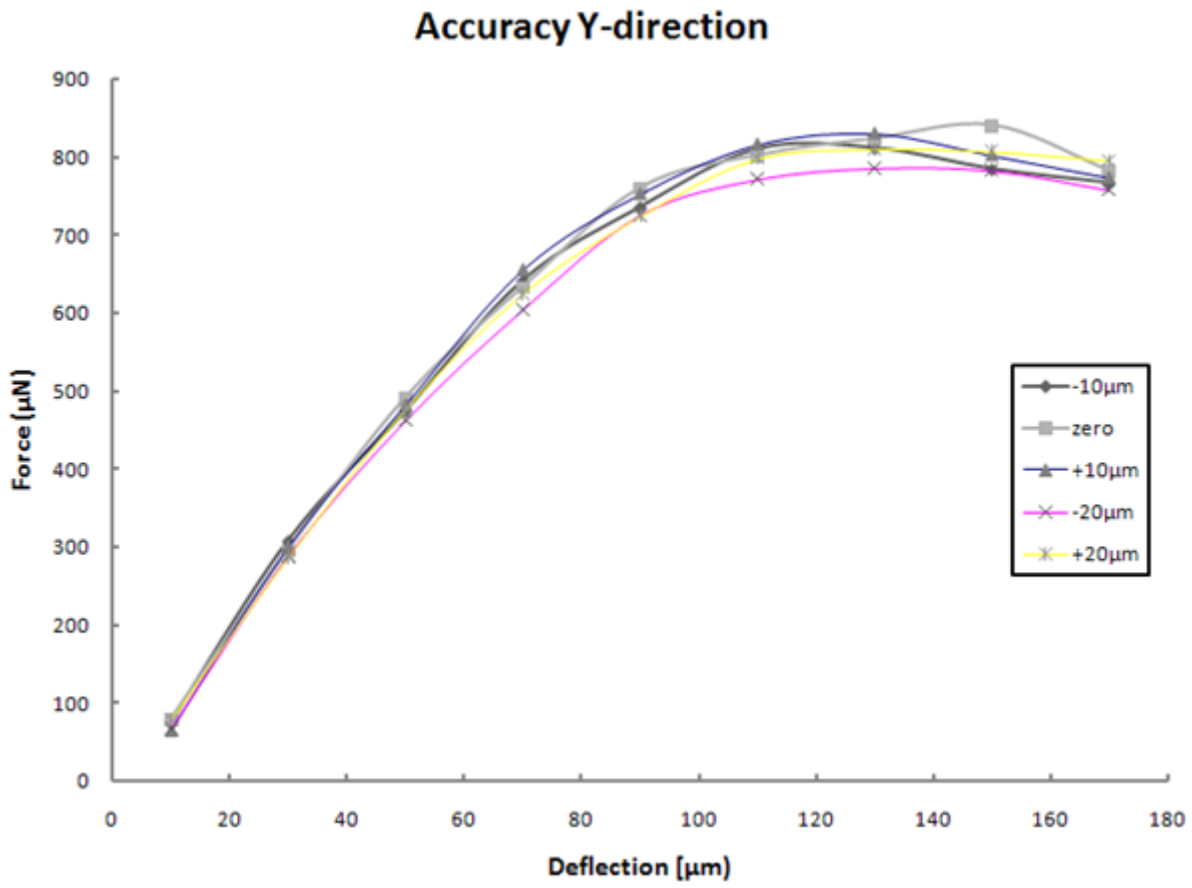

Figure 7-2: Stylus placement accuracy Y-direction.

In the plot it is shown that the difference between the results increases with increased deflection. Because of symmetry the measurements ±10 µm should be approximately equal and also the measurements ±20 µm. The only measurement which stands out a little is the -20 µm measurement which seems to have values a little below the others. However a placement error of ±20 µm is much larger than expected error when placing the stylus with the help of a microscope. With structures of the size of the SW412 and a magnification of 90x on the microscope I would estimate the stylus placement accuracy to be within ±5 µm in the X- and Y-direction. This deviation is small compared to the measurement series intervals done in Figure 7-2.

Since most of the points of the measurements -10µm, zero and +10µm are inside the expected standard deviation of 6.8 µN from Chapter 6.1 “Signal from loadcell”, I conclude that with placement of the stylus through a microscope in the Y-direction the error of placement from centre of mass have negligible

effects on the measurement result. The reason that the effect is so small is because the width of the spring is 80 µm, so the error of placement is well inside this width. Also because of the spring it is easy to place the stylus in the y-direction since the spring can be used as a reference point to aim after through the microscope.

7.1.2 X-direction

I have done similar measurements in the x-direction, but I only did three different measurements, -10 µm, zero and +10 µm. The results are shown in Figure 7-3.

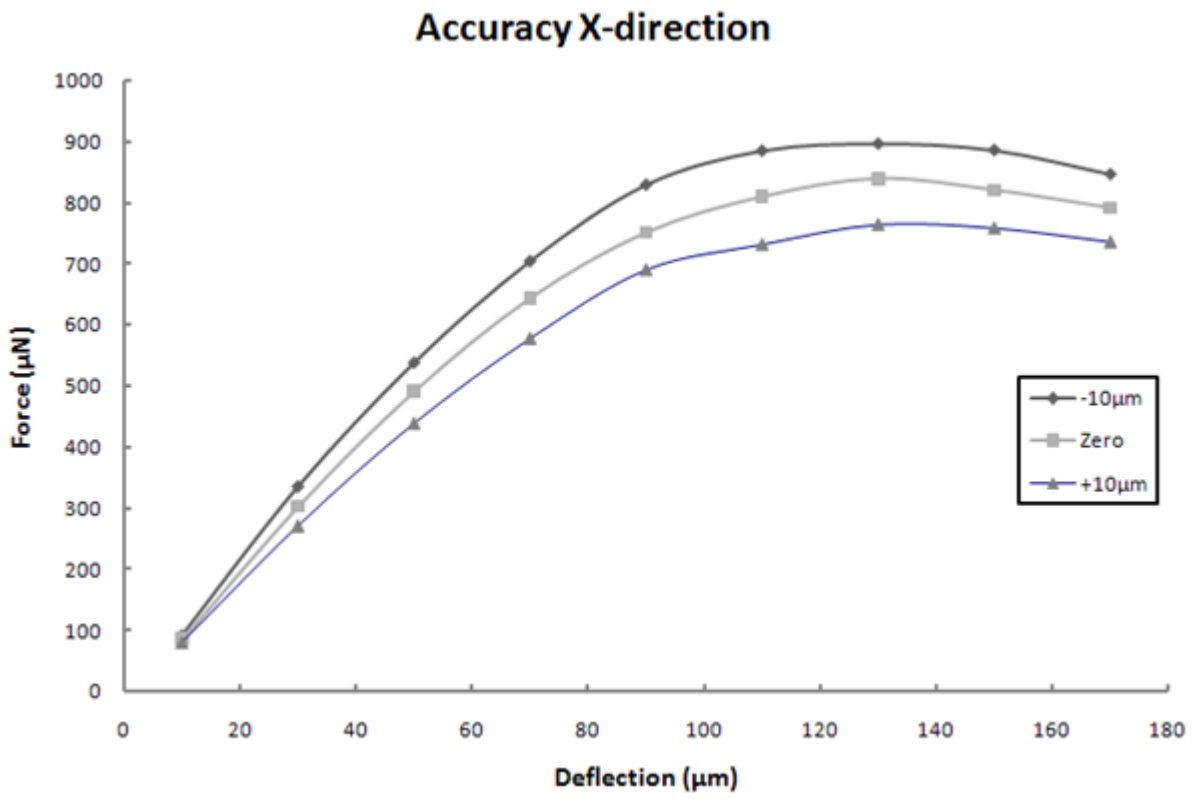

Figure 7-3: Stylus placement accuracy X-direction.

This measurement shows a different behavior from the one in the y-direction. From the calculations of the spring constant along the mass from Chapter 2.2 “Deflection” this was expected. This behavior will also be studied closer in a later chapter where the spring constant along the mass is measured (Chapter 7.3). The spring constant in the linear area of each of the measurements in Figure 7-3, are shown in Table 7-1. This is simply the slope of the curve in this area.

Table 7-1: Spring constant.

-10µm	10.2 N/m
Zero	9.3 N/m
+10µm	8.3 N/m

From Table 7-1 it is found that for 1 µm error of stylus placement in the X-direction the spring constant in the linear area will deviate with approximately 0.1 N/m in the force/deflection measurement. There will also be a deviation in the curved area of the curve as seen in the figure.

7.2 Analysis of the force/deflection curve shape

In Chapter 5 “Initial measurement” the shape of force/deflection curve was commented. In this chapter the curve shape is analyzed more thoroughly. On different parts of the curve different phenomena decides the shape of the curve. In Figure 7-4 the curve is roughly divided in to three parts. In the first part of the curve {1}, there is a somewhat linear relationship between the force and deflection. In the second part of the curve {2} the force is first diminishing and then reducing as the deflection increases. In the third part {3} some unexpected behavior arises as the structure is approaching fracture. In the following subchapters each part of the curve is discussed.

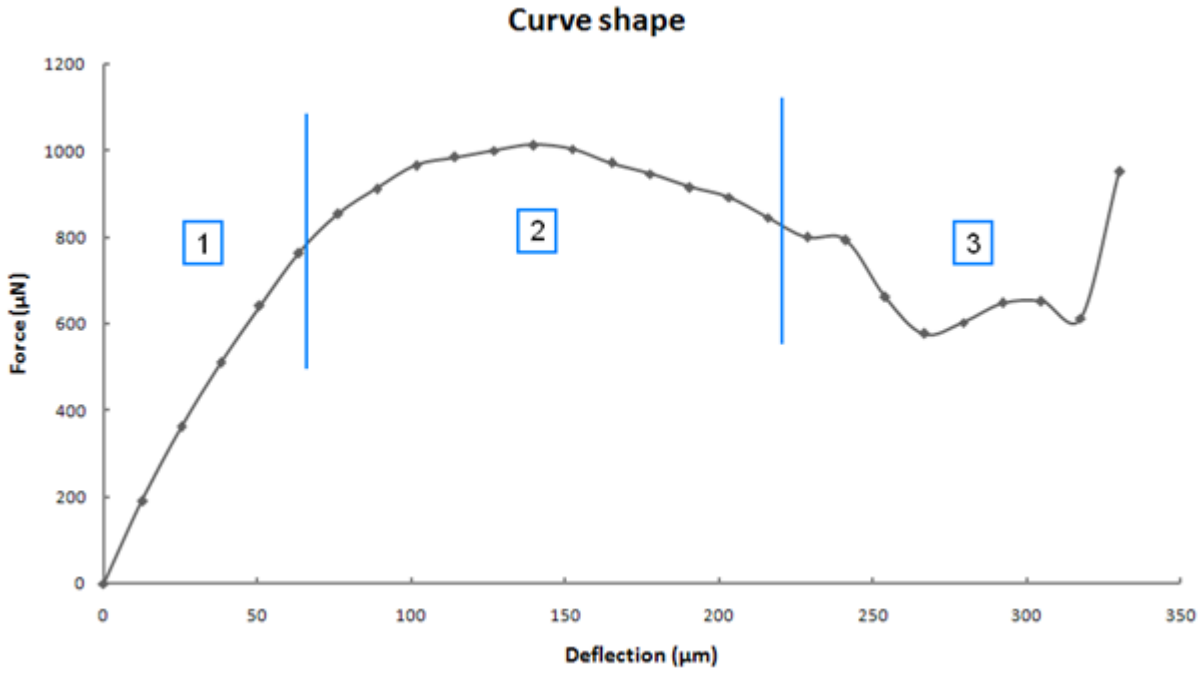

Figure 7-4: Force/deflection curve divided into three regimes.

7.2.1 Linear regime {1}

The provided SW412 accelerometer structures are made of silicon. Silicon is a material that is very elastic and brittle. These material properties yields that structures made of silicon experience very little or no plastic deformation before fracture. Knowing this, the expected behavior of the curve would be a linear relationship between the force (F) and the deflection (x) until fracture. This would be true if only the material properties determined the properties of the structure. However geometrical properties in the structure, often nonlinear, also decide the structures properties. Of various reasons discussed in the next subchapter a linear behavior is not the case in the whole range of this measurement. However in part {1} of the curve in Figure 7-4 there is a somewhat linear relationship which can be expressed as F=kx, where *k* is the spring constant. In the first part of the curve {1} this spring constant can simply be found by finding the slope of the curve.

7.2.2 Curved regime {2}

As the deflection increases the relationship between the force and deflection is no longer linear. The curved regime of the curve {2} is entered. In this regime the force diminishes as the deflection increase, and after this the force also decreases as the deflection increase further. There are a few different reasons for this behavior. Two of them are shown in Figure 7-5.

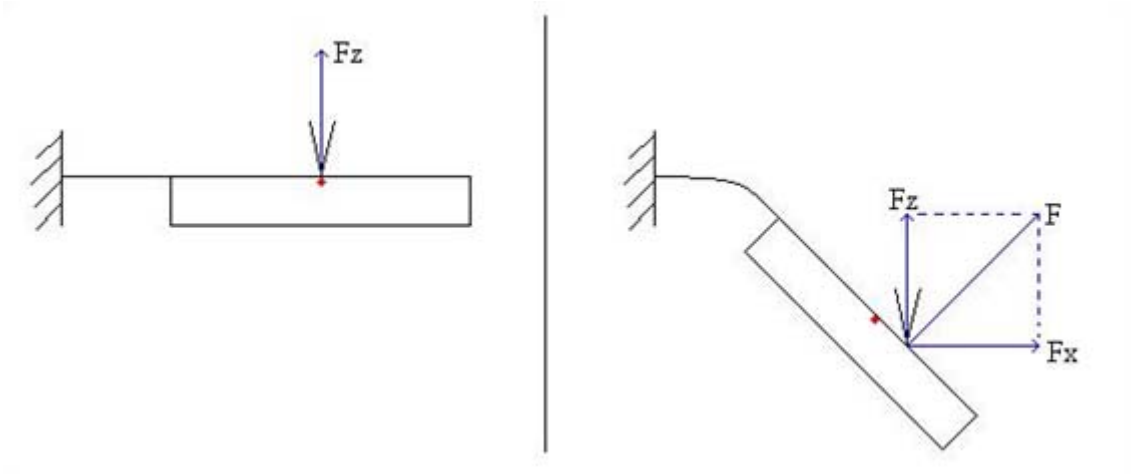

Figure 7-5: Nonlinear effects on curve shape.

As seen on the left in Figure 7-5 the Fz force will be approximately equal to the perpendicular force F on the mass with small deflections. At larger deflections, as shown on the right, Fz and F are no longer equal. With the measurement setup built it is only possible to measure the Fz force and not the F force which will be bigger than Fz at larger deflections. So even though the measured Fz force decreases as the mass deflects the actual force F perpendicular to the mass surface increases. This is one reason the curve in Figure 7-4 is not linear.

Another reason is also shown in Figure 7-5. The stylus can only be moved in the z-direction during a measurement, it cannot be moved in the x- or y-direction. As the measurement starts the stylus is placed at the centre of the mass, indicated with a red dot in the figure. As the structure deflects the stylus will start to slide on the mass, and no longer be in the centre of mass. As discussed in Chapter 2.2 “Deflection” the spring constant at this point will be lower than the one at the centre of mass. Therefore a lower force is needed to deflect the mass at this new point. This is another reason why the force is decreasing at high deflections, and the curve in Figure 7-4 will not be linear until fracture.

Another reason is because the stylus is not perfectly sharp, it has a given radius discussed in Chapter 2.3 “Stylus tip size”. This will cause a rolling effect similar to the sliding effect discussed above. However this effect will be relatively small compared to the previous effects. The rolling of the tip can only move the point of applied force with maximum the radius of the tip (17.78 µm). This is a relatively short distance compared to how far the stylus can slide along the mass (half the length of the mass, 93 µm, if the stylus is placed on the centre of mass when starting the measurement).

To try to eliminate these effects I have made some calculations on a measurement and taken into account that the Fz and F are not equal, and that the stylus slides along the mass. In this calculation I have simplified the deflection of the spring to only a deflection at the point where the spring is supported. This was done to be able to use simple geometric considerations. I have transformed the measured Fz force to a force perpendicular to the mass. And I have assumed constant torsional stiffness around the point of deflection, corresponding to the spring constant at the point where the force attacks. In Figure 7-6 the result of the calculation is shown.

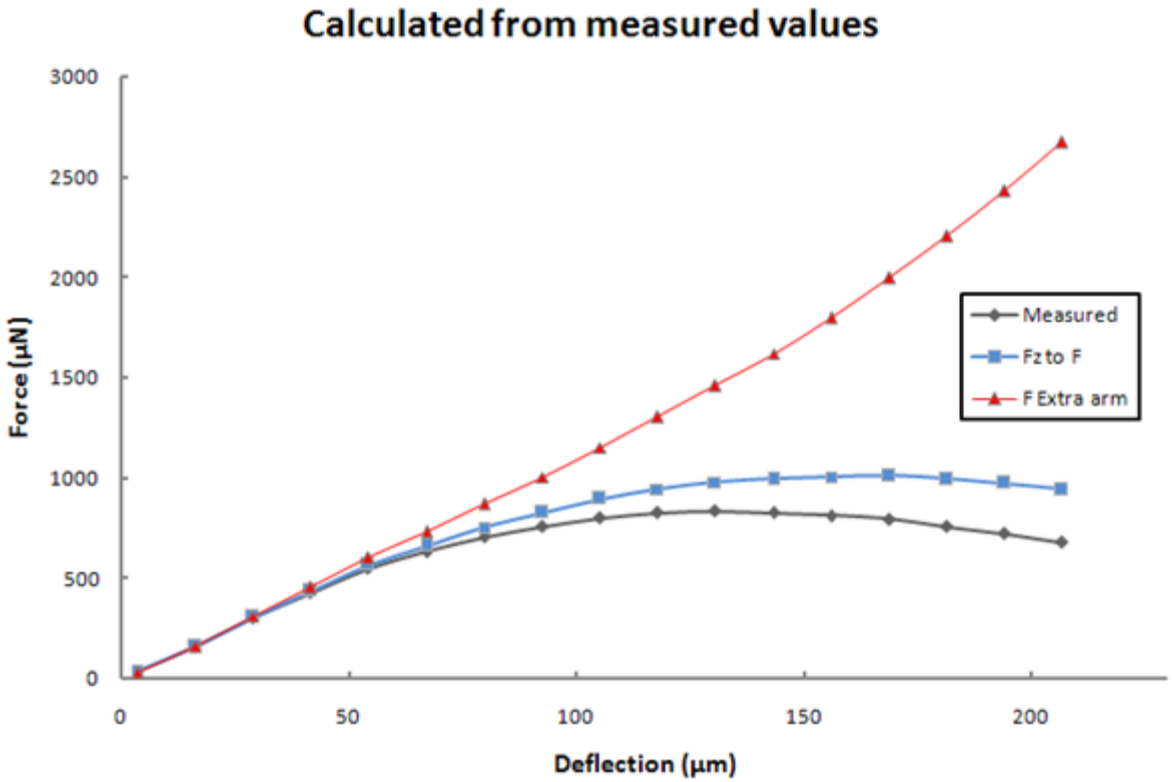

Figure 7-6: Calculated linear curve from measured series.

In Figure 7-6 a force/deflection measurement is performed on a structure with the stylus placed at the centre of the mass. The measured Fz values of the force/deflection measurement are the black curve. In the blue curve the measured value of Fz is used to calculate F (Figure 7-5, Equation 7.1) the perpendicular force on the mass. And in the red curve the extra arm of the measurement when the stylus slide along the mass is compensated (Equation 7.2). Some simplifications are done in the calculation, and the red curve in Figure 7-6 is not exactly linear, but the figure illustrates the expected linear relationship between the force and deflections in silicon structures, as explained in Chapter 7.2.1. “Linear regime”.

The formula to transform z-force to force perpendiculear to mass:

$$F = \frac{Fz}{\cos\left(\arctan\left(d/214\mu m\right)\right)} \tag{7.1}$$

Formula to compensate for the extra arm:

$$F_{extra\ arm} = F + (0.1\ \mu N/\mu m/\mu m * y * d) \tag{7.2}$$

Where:

$$y = \sqrt{(214\mu m)^2 + d^2} - 214\mu m \tag{7.3}$$

In the equations *d* is the measured value of deflection shown on the x-axis of Figure 7-6. 214 µm is the distance from the centre of the mass to where the spring is fixed, and *y* is the distance the stylus slides along the mass. The value 0.1µN/µm/µm is the slope of the spring constant from centre of mass to the end of the mass (in this area the slope is not linear, but it is used as an approximation). The value was found in Chapter 7.1.2 "X-direction". Another simplification done is that when finding the slope of the mass on the structure it was assumed that all deflection of the spring was done in the supported end. This simplification was done because simple geometrical considerations could then be used, and since the mass is so much longer than the spring this will not have a big influence on the calculation.

7.2.3 End regime {3}

When the structures exceed deflections of approximately 220 µm, when they are loaded at the centre of mass, they go from the curved regime {2} to the third regime {3} of the curve in Figure 7-4. In this regime the structures are close to fracture and in Figure 7-4 we see that the curve is no longer smooth, it has some irregularities. What happens with the structures that yields this behavior of the curve in this regime will be discussed in Chapter 7.4 "Destructive tests".

7.3 Spring constant along mass

In this measurement I have done 13 different measurements along the mass on structure A1, in the linear regime of the force/deflection-curve. The placement of the stylus along the mass is shown in Figure 7-7.

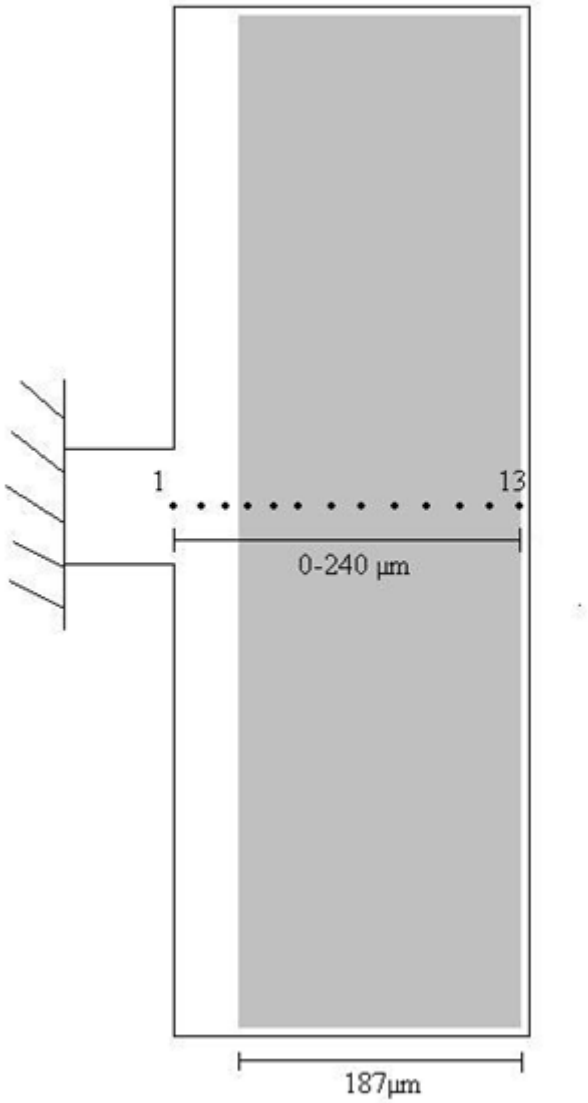

Figure 7-7: Placement of stylus along mass

In each of the 13 measurements I have done 3-4 force/deflection-measurements in the linear regime. The distance between each force/deflection-measurement on the mass is then 20 µm. The results are shown in Figure 7-8.

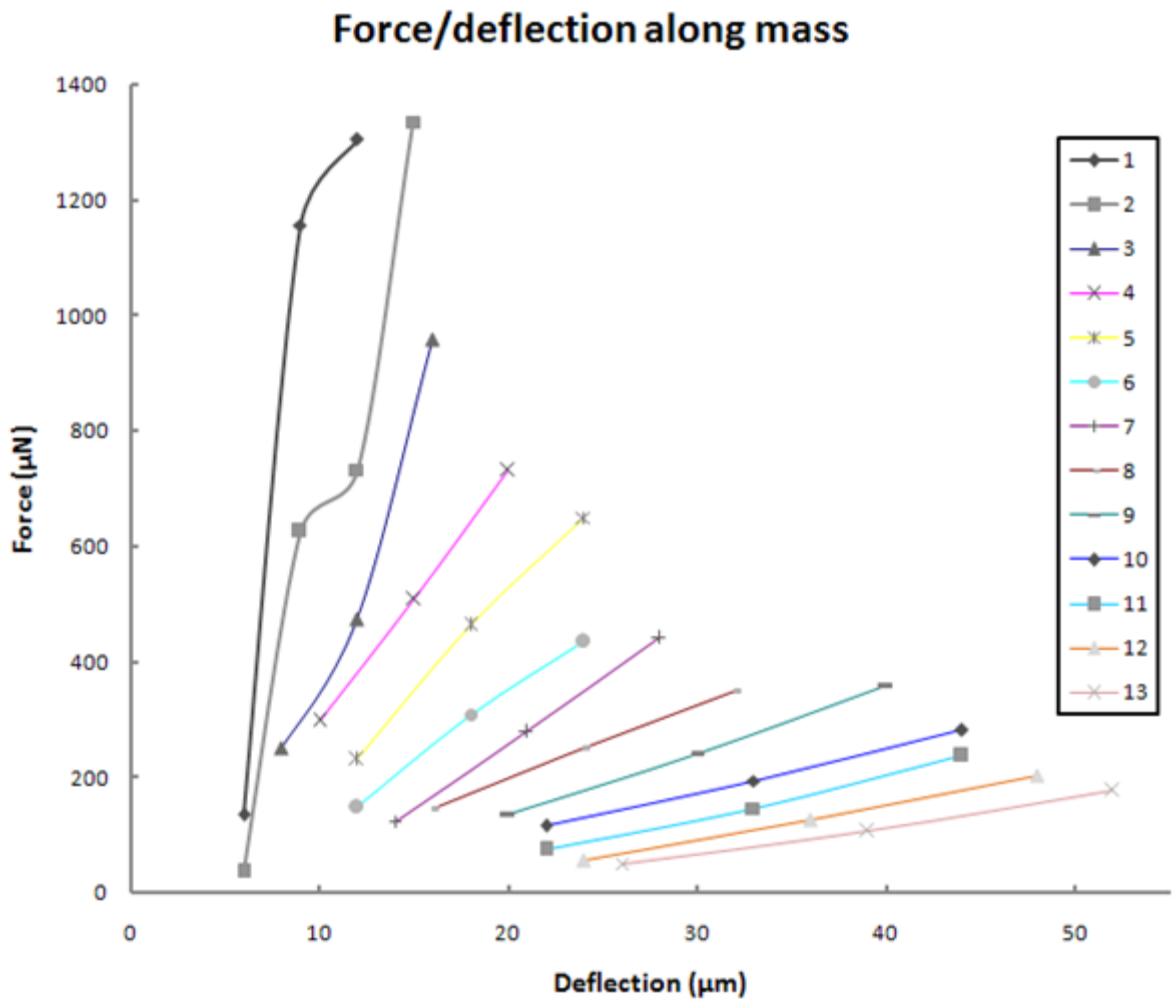

Figure 7-8: Force/deflection along the mass in the linear regime.

As seen in the Figure 7-8 measurement 1-3 does not appear to be in the linear regime. As seen in Figure 7-7 these points are not on the actual mass (shaded area) of the structure, but on an area of equal thickness as the spring (3.2µm) in front of the mass. These three measurements are also in the linear regime, but the microstep error discussed in Chapter 6.2 “Actuator precision” comes in to play because the deflection interval in these three measurements is so small.

By calculating the slope of each of the thirteen measurements the spring constant is plotted along the mass. For the three nonlinear measurements an approximation of the slope is done. So the plot of the spring constant shown in Figure 7-9 is actually the spring constant on the plate area in front of the mass, and on the mass (as shown in Figure 7-7, 0-240 µm).

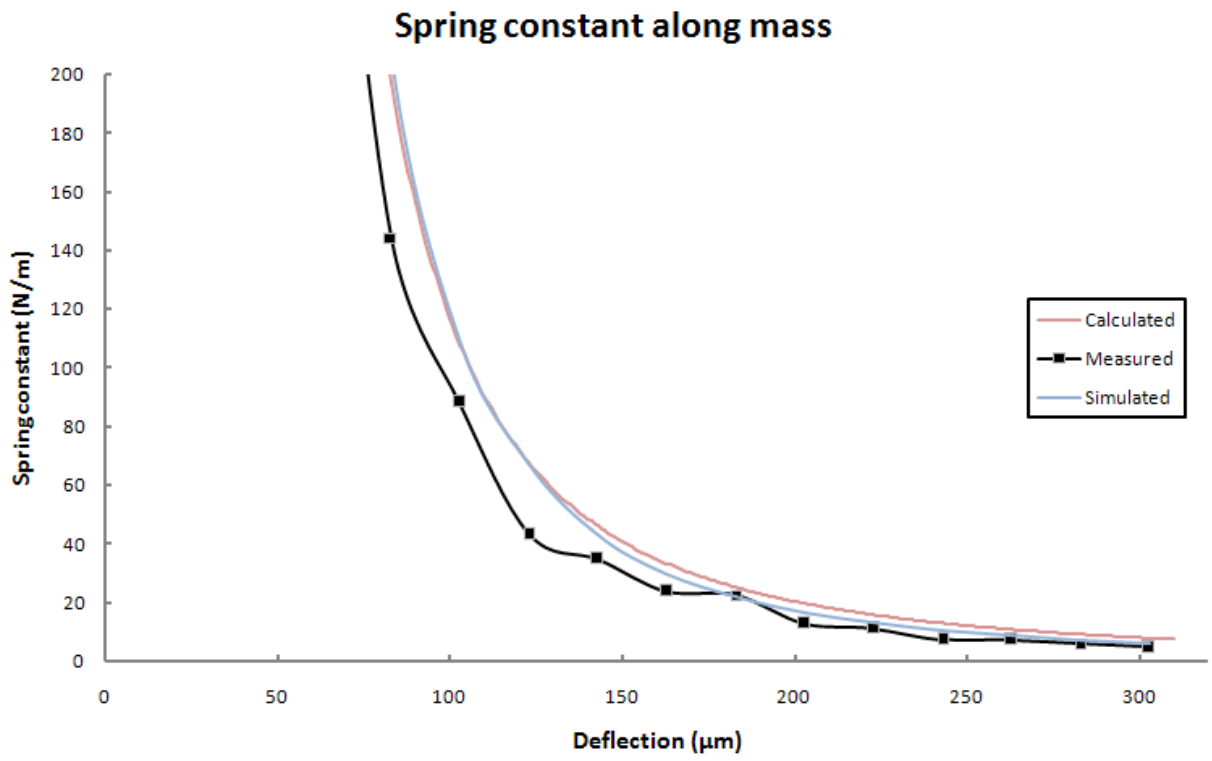

Figure 7-9: Spring constant along the mass

In Figure 7-9 the black curve is the spring constant found from the measurements. The black dots on the line represent each of the thirteen measurements. The red and blue curves are the calculated and simulated values of the spring constant. The calculated values are based on the same results shown in Equation 2.7 and 2.13 and Figure 2-6, only the plate area between the spring and the mass, shown in Figure 7-7, are taken into account. This plate area was not known when the calculations in Chapter 2.2 "Deflection" were done in the beginning of the project. For details of the calculation see Chapter 2.2.

For the simulation a simple model of the structure was made using Ansys. A sphere with a radius equal to the stylus tip radius was placed on the mass to simulate the stylus. The deformed shape of the model with the sphere is shown in Figure 7-10.

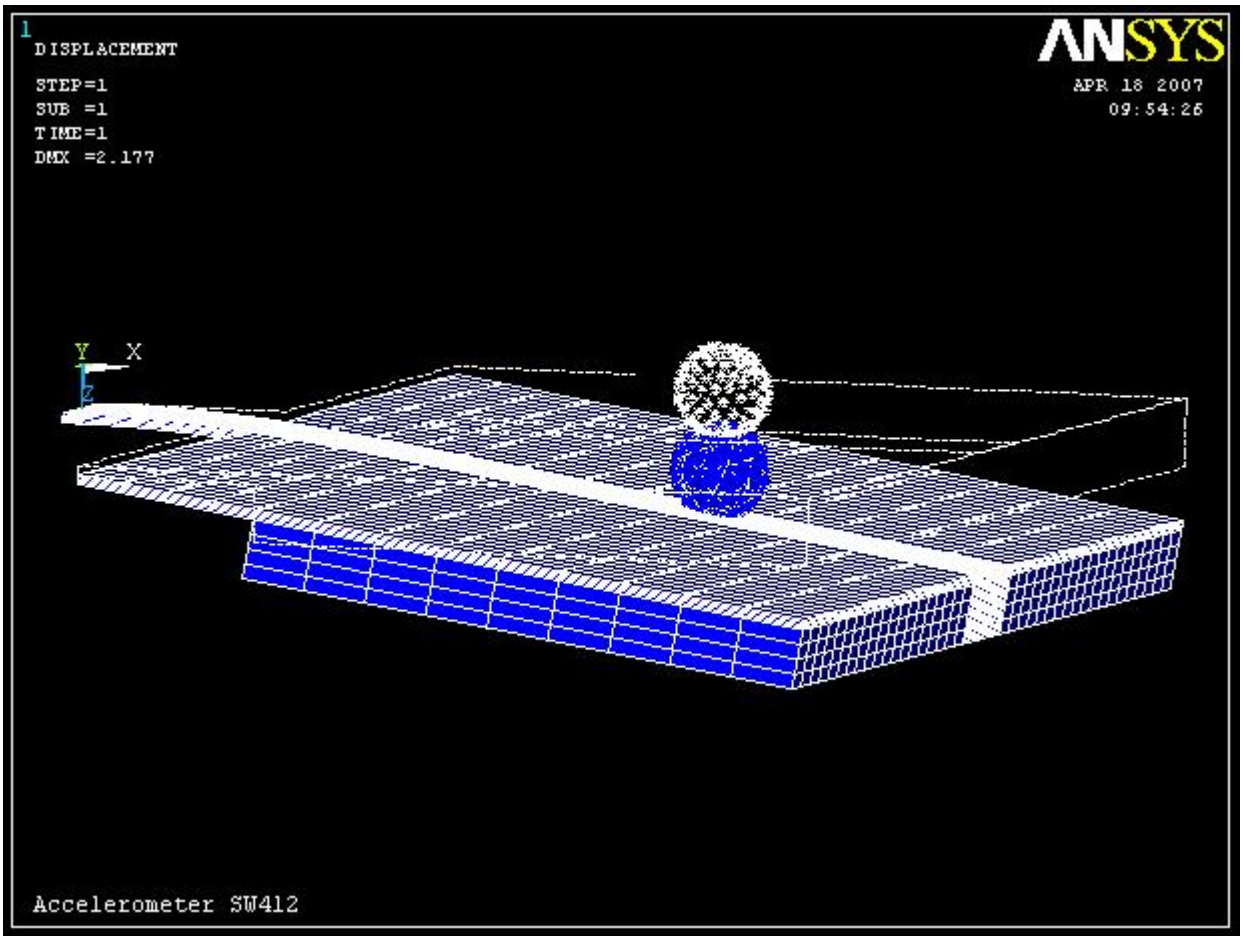

Figure 7-10: Simulation model, deformed shape, with undeformed edge.

In the simulation the model was fixed at the support of the spring, and constraints on the sphere was that it could not move in the x- and y- direction, it could only move in the z-direction. A small force was applied to the sphere, and by contact simulation[1] between the sphere and the model this force was transferred to the model of the structure. Compared to the model the sphere will not deform, all the deformation will be done on the modeled spring. So the displacement of the nodes in the sphere will be equal to the deflection of the stylus tip. From the force applied and the displacement of the nodes the spring constant is found. To plot the simulated spring constant along the mass, the sphere is moved along the mass (similar to Figure 7-7), and the simulation is repeated.

As seen in Figure 7-9 the measured and analytical curves are not that different. The analytically calculated and simulated values are almost similar, while the measured differ some from the analytical. Reasons for this deviation can be that the N-well profile at the edges of the mass is not taken into account in the calculation and simulation. The N-well is what defines the mass and it gives a gradual

[1] The reason for the use of the rather advanced contact simulation instead of just applying force on different nodes of the model, was that initially the simulation was intended to verify the whole range of the force/deflection curve. This was not accomplished because at large forces and deflections the solver would not converge.

transition between the spring and the mass. In the calculation and simulation a simple box model of the structure is used. Also an assumption that the spring is perfectly clamped is made in the calculation and the simulation, in real life the spring is not perfectly clamped. Despite this the curves in Figure 7-9 are not that different.

7.4 Destructive tests

7.4.1 Fracture measurements on six different structures

I have performed a series of destructive tests on some of the SW412 accelerometer structures. The results of these tests are shown in Figure 7-11.

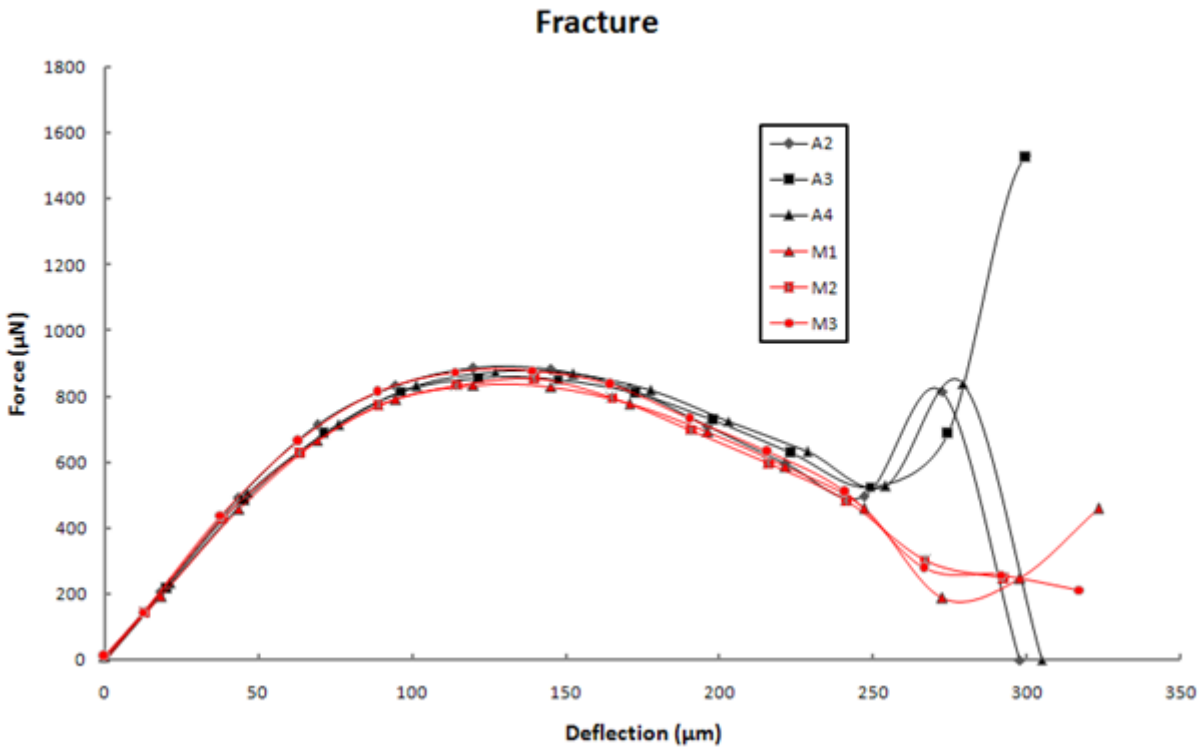

Figure 7-11: Fracture test on six different structures

In Figure 7-11 six different structures , A2-4 and M1-3, are tested at the centre of mass. Only two of the structures actually experienced fracture, this was structure A2 and A4. The A-structures and the M-structures are positioned on opposite side of the wafer. Therefore the loadcell and stylus was rotated 180 degrees with respect to the wafer, this is discussed closer in Chapter 7.4.4 “Fracture tests with different loadcell position”.

Up to deflections of 250 µm the curve shows the expected behavior described in Chapter 7.2 “Analyzis of the force/deflection curve shape”. At deflections higher than 250 µm the curve shows an unexpected behavior. The force is now increasing, which is not what would be expected. One possible reason for this unexpected behavior could be the geometry of the stylus. The stylus has been studied under a microscope and approximate dimensions have been measured. The geometry and dimensions of the stylus are shown in Figure 7-12.

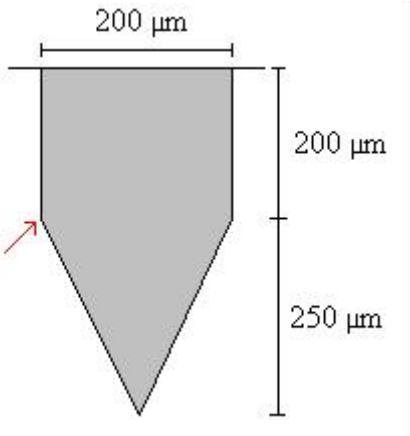

Figure 7-12: Stylus dimensions

As seen in the figure the actual tip is 250 µm long. So a reason for the increasing force at approximately 250 µm deflection might be that the corner of the stylus, shown with an arrow in Figure 7-12, comes in contact with the structure.

To try to confirm this theory some tests were performed with the stylus placed closer to the spring than the centre of mass where the previous tests in Figure 7-11 was taken. Closer to the spring it will take smaller deflections to reach fracture, therefore the corner of the stylus is not expected to come in contact with the structure. Results from these measurements are shown in Figure 7-13, together with the results from Figure 7-11.

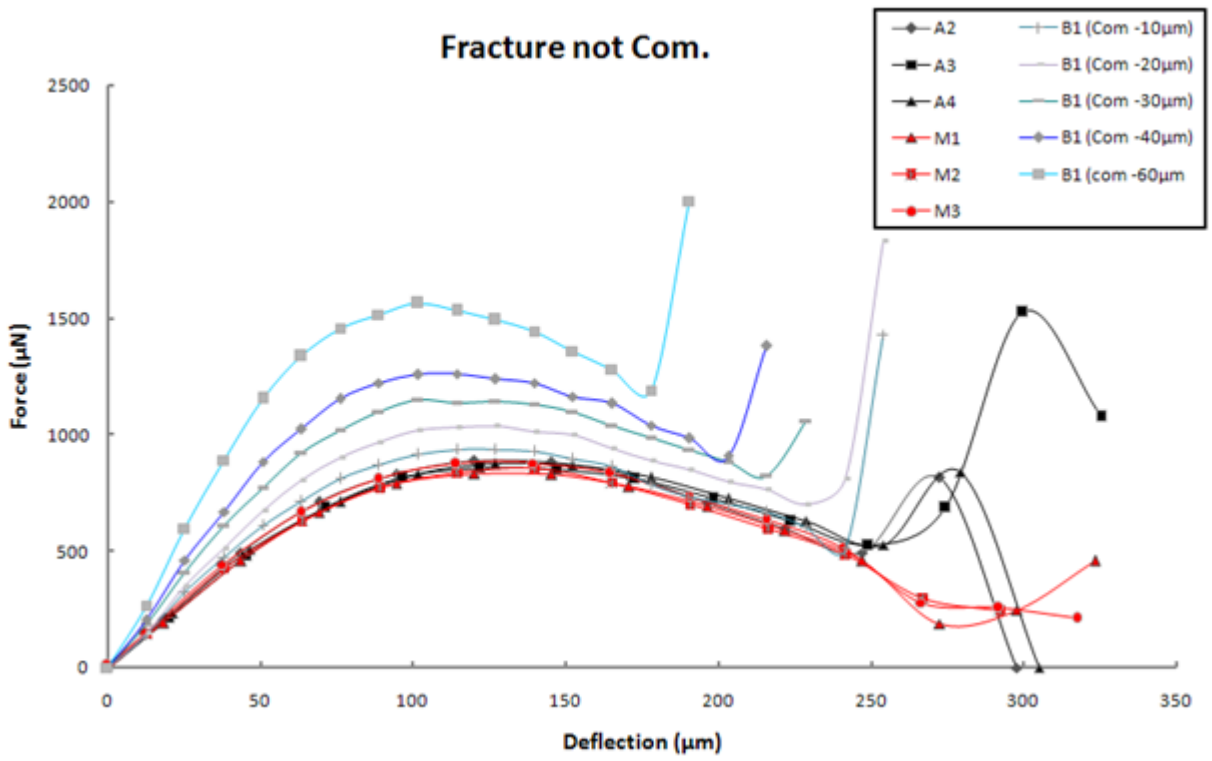

Figure 7-13: Fracture test not on the centre of mass

In Figure 7-13 the A and M measurements are the same as before and in these measurements the stylus is initially placed at the centre of the mass. The other measurements are on structure B1, and the stylus is placed closer to the spring with the given distances. As seen the behavior of increased force readout as the structure is close to fracture is still present. The deflections needed to reach the point where the force is increasing, is decreasing as the stylus is placed closer to the spring. When the stylus is placed 60 µm from the centre of mass, a deflection of approximately 180 µm is needed. At this deflection the corner of the stylus is not even close to the structure, so I conclude that the corner touching the structure is not the reason for the unexpected behavior. This behavior is studied closer in the next subchapter 7.4.2 “Fracture measurements with pictures”.

7.4.2 Fracture measurement with pictures

To study the behavior of the curve further I decided to cut a wafer along the gap beside the mass. This way the measurements could visually be studied “live” straight from the side through a microscope. In Figure 7-14 the measurement results of such a measurement are shown, the stylus is placed at the centre of mass.

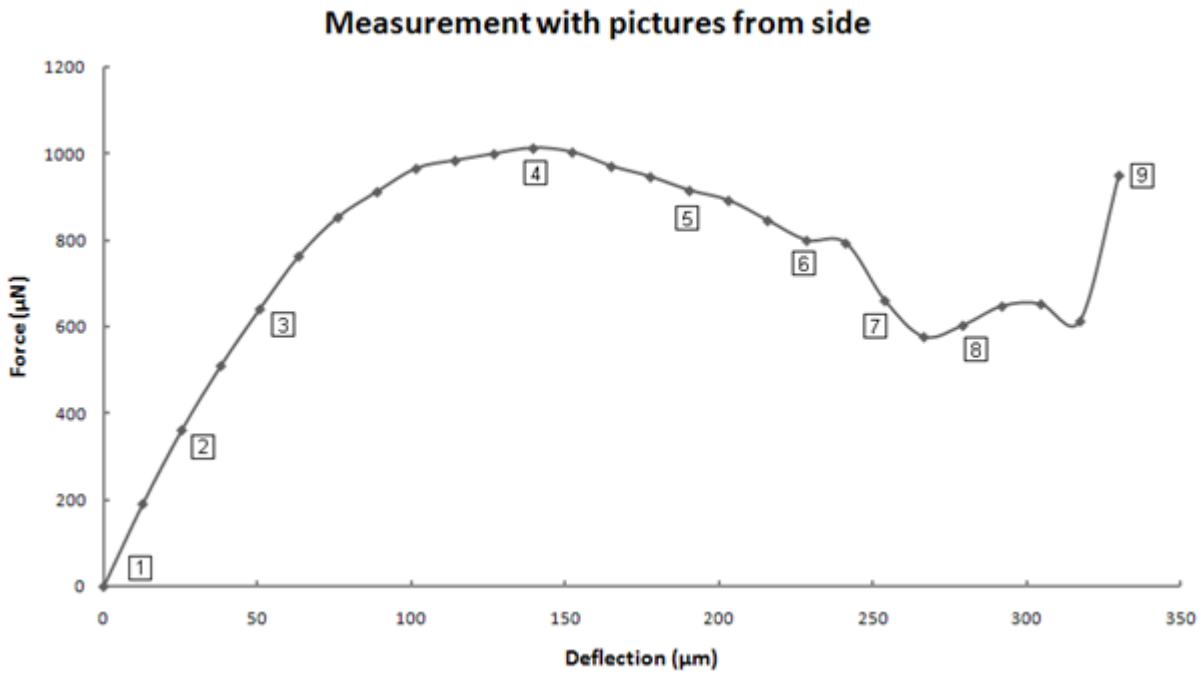

Figure 7-14: Measurement with pictures. (Point number in square brackets.)

In Figures 7-15 – 7-23 pictures from the measurement corresponding with the point numbers in Figure 7-14 are shown.

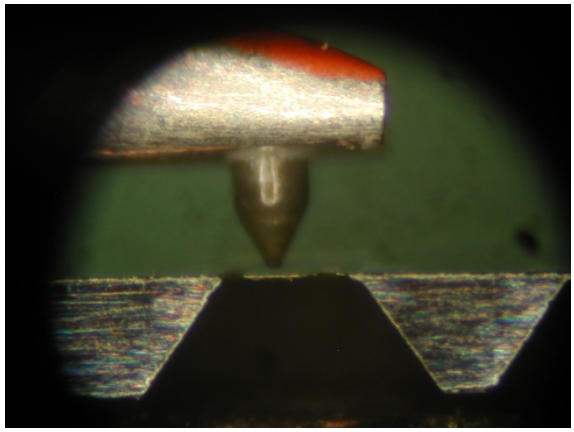

Figure 7-15: Point 1

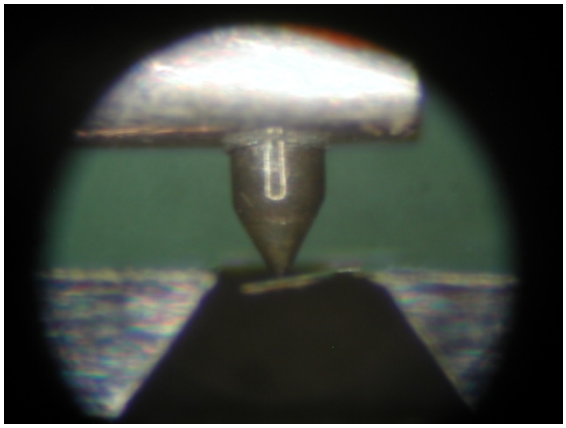

Figure 7-16: Point 2

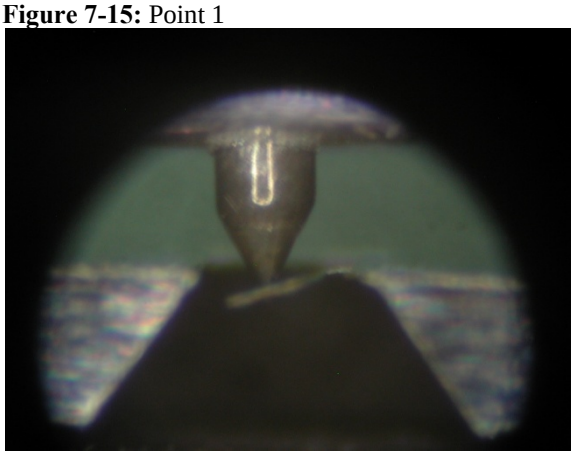

Figure 7-17: Point 3

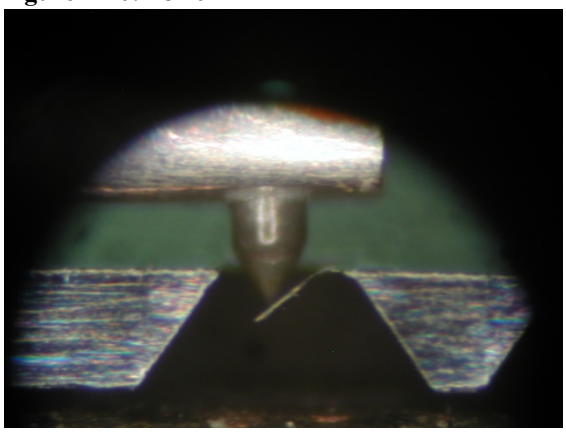

Figure 7-18: Point 4

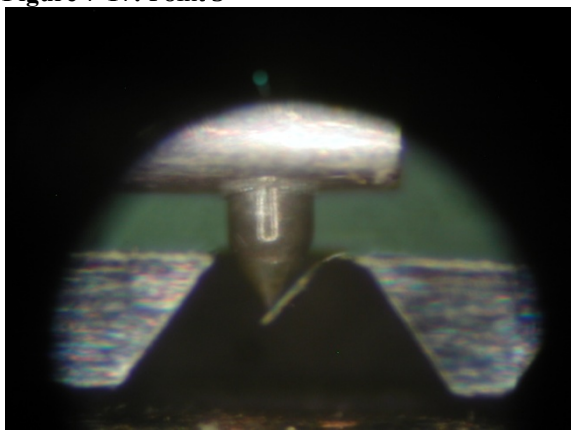

Figure 7-19: Point 5

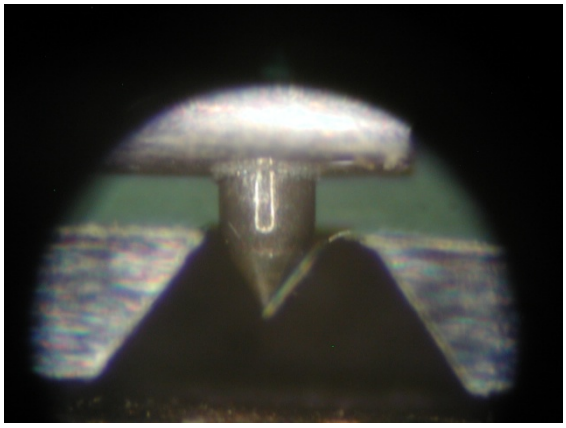

Figure 7-20: Point 6

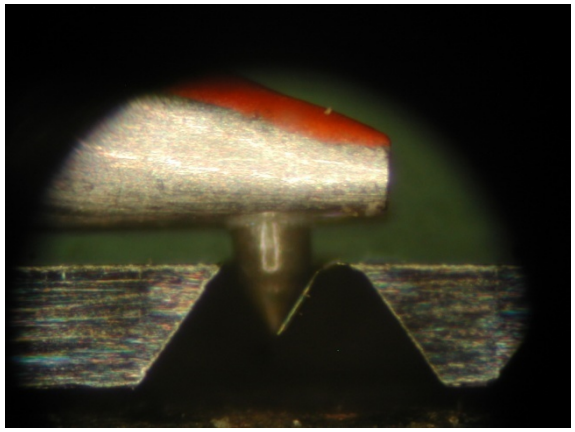

Figure 7-21: Point 7

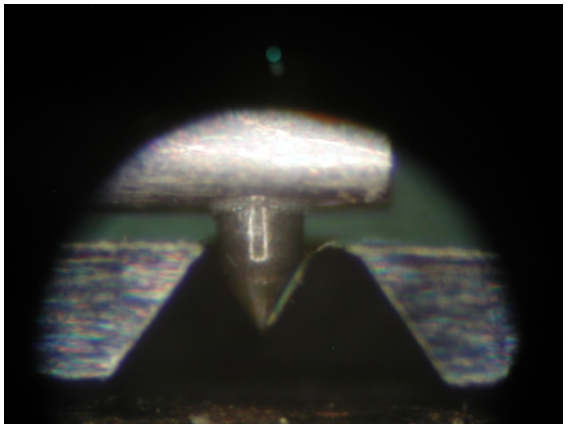

Figure 7-22: Point 8

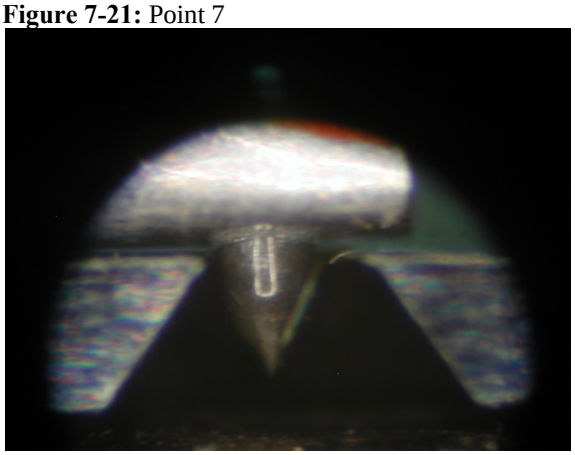

Figure 7-23: Point 9

Figures 7-15 – 7-32 show the position of the structure at different points of the measurement. In the Figure 7-14 there is a "bump" in the measurement between point 6 and 7. As it looks in the microscope this comes from the end of the mass sliding off the stylus tip. After point 7 the graph flattens. The reason for this seems to be that the slope of the mass is equal to the slope of the stylus, so the mass is parallel to the slope of the stylus.

The reason for the increase in force at point 9 is still not easy to spot. In point 9 it almost seems like the silver colored structure in which the stylus is attached is touching the surface of the wafer. This would however not explain the curves of structure B1 in Figure 7-13, because in that measurement the deflections are smaller. It is not so visible in the figures, but in the microscope it is easier to see what happens with the structure after point 7. As the mass slides in parallel with the stylus the point of attack of the force gets closer and closer to the spring, and as it reaches the spring the measured force will increase because the spring constant of the spring is much larger than the one of the mass (as discussed in previous Chapters 2.2 "Deflection" and 7.3 "Spring constant along mass"). This is the reason why there is an increase in the measured force values in the end of the curve. If the structure was deflected further the structure would fracture because with the suddenly increasing spring constant small deflections will give large forces on the structure.

7.4.3 Fracture test with stylus closer to spring

To reach fracture at smaller deflections the stylus could be placed closer to the spring relative to the center of the mass. It would be interesting to see if the same effects seen in the figures and commented in the previous subchapter would come in to play when the stylus is placed closer to the spring. In Figure 7-24 the stylus is placed 50 µm closer to the spring from the centre of mass. Pictures are not shown for this measurement, but the measurement was monitored from the side through the microscope.

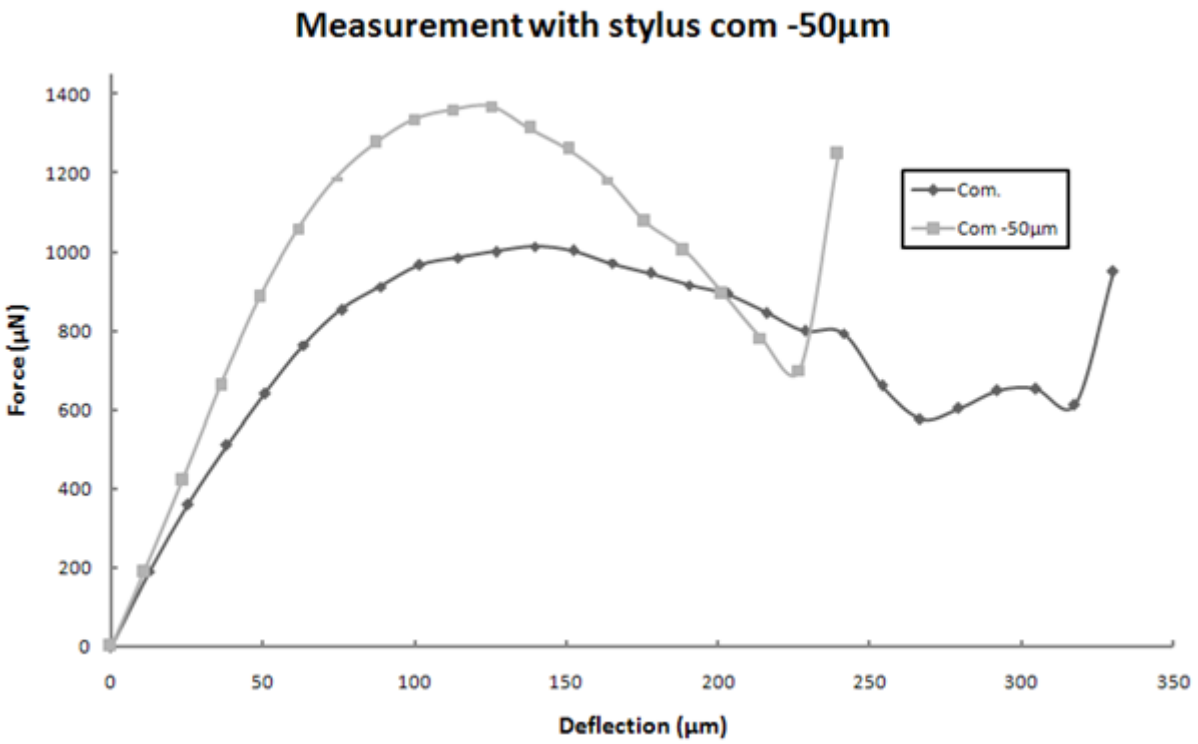

Figure 7-24: Force/deflection measurement with stylus placed closer to spring.

In Figure 7-24 the original measurement with the stylus placed at the centre of mass is shown together with the measurement with the stylus placed 50 µm closer to the spring. The figure shows that the slope is different in the linear regime for the two curves, as discussed in Chapter 7.2 and 7.3. Since the stylus is placed closer to the spring the stylus has a longer distance to slide before it slides of the mass. In fact the stylus will not slide of the mass before the structure fractures, and therefore the "bump" seen in the original measurement will not exist in the measurement closer to the spring. What is similar in the two measurements is that the force is increasing right before fracture. From this we learn that even with placing the stylus closer to the spring, the mass will be in parallel with the stylus before the structure fractures. The reason for this is that the mass is rigid, so that the slope of the mass will be the same right before fracture no matter where you choose to place the stylus on the mass. If the stylus was placed on the spring the slope would be different. But because of the relatively small deflections of the spring compared to the mass other factors such as placement accuracy of the stylus (discussed in Chapter 7.1

“Stylus placement accuracy simply supported mass”) and resolution of the deflection (discussed in Chapter 6.2 “Actuator precision”) will come much more in to play.

7.4.4 Fracture tests with different load cell position

In the three black A-measurements, in Figure 7-11, the stylus and load cell were placed along the spring and on to the mass. In the three red M-measurements the load cell and stylus was rotated 180 degrees, as shown in Figure 7-25. This was done to study if there were any significant differences in the measurements between the two positions. As seen in Figure 7-11 the difference between the red and the black curves are minimal in the linear regime of the curve. In the curved regime of the curve there is a little difference between the black and the red curves. The reds seem to lie a little lower than the blacks. This is because of the Fx-force previously discussed and shown in Figure 7-5, and also shown in Figure 7-25. The x-force gives an extra moment on the stylus which adds or subtracts to the measured force depending on which way the load cell and stylus are positioned. For the three black measurements the moments adds a force, and it subtracts from the three red measurements, hence the small difference in the curved regime.

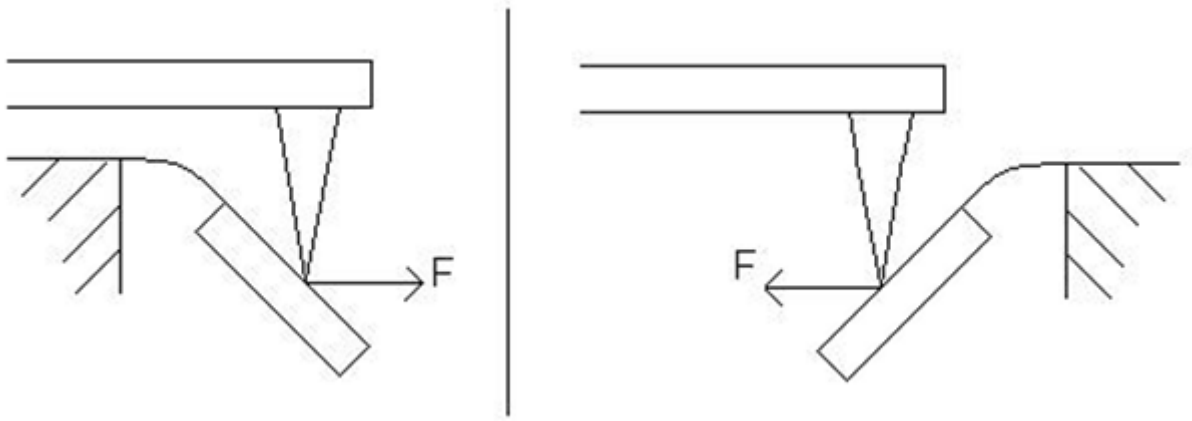

Figure 7-25: Moment on tip of stylus.

As seen in Figure 7-11 there is a significant difference between the red and the black measurements at deflections above 250 µm. The reason for this is that the stylus is not perfectly aligned. In this regime of the curve the slope of the structure is in parallel with the slope of the stylus, as discussed in Chapter 7.4.2 “Fracture measurements with pictures”. When the stylus is not perfectly aligned the slope of the stylus will be different on each side. If the structures are deflected further Figure 7-25 shows how the structure will be in parallel with one side of the stylus with the black measurements, and the other side for the red measurements. The difference between the red and black curves with deflections above 250 µm in Figure 7-11, comes from the different slope of each side of the stylus because it is not perfectly aligned.

7.4.5 Conclusion destructive tests

As a conclusion on the destructive tests of the SW412 I would say it would be difficult to perform fracture testing on this structure with the current measurement setup. The reason for this is the geometry of the measurement stylus combined with the big deflection and slope the structure experiences before fracture. The slope of the structures when it would fracture is actually bigger than the slope of the stylus, so the mass and stylus will be in parallel before fracture. The force is then no longer a point load and it is difficult to analyze.

The behavior up to fracture of the structures to be tested will heavily depend on the geometry of the structures. Other simply supported mass structures might not have so big slope on the mass before fracture is reached. Then the stylus might not slide of the mass, and the sudden increase in force before fracture will not occur because the mass is never in parallel with the stylus.

Fracture tests have also been performed on another accelerometer design which is not so flexible. This structure is also simply supported, but it has two springs on one side of the mass, as shown in Figure 7-26. This design was made in the MPW process by the PhD. student Craig Lowrie, in connection with the heart wall motion monitoring project at VUC [15]. Because the two springs are fixed with so big distance between them the stylus placement accuracy in the y-direction shown in Figure 7-1 will not be an issue.

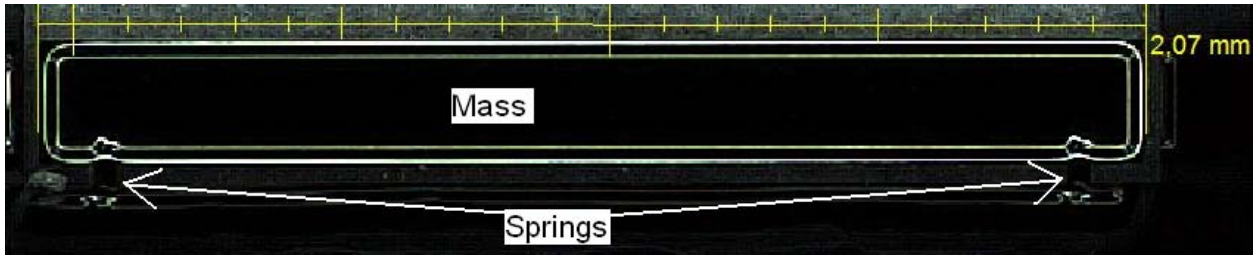

Figure 7-26: Craig-design accelerometer structure.

On the Craig design the force/deflection curve is a little different from the measurements done on the SW412 structure. The measurement results of two different measurements performed on the Craig-design at the centre of mass are shown in Figure 7-27. As seen in the figure larger forces are measured than on the SW412 structure, approximately 4000 µN for the Craig-design versus approximately 900 µN for the SW412. The spring constant at the centre of mass of the linear regime of the curve is approximately 61 N/m and 66 N/m for the two different measurements on the Craig-design. Compared to the SW412 approximately 10 N/m spring constant we see that the Craig-design is a lot stiffer. We also see in Figure 7-26 that the structure fractures at approximately 115 µm deflection. The “bump” before the fracture is probably the end of the mass sliding of the tip of the stylus as discussed earlier in Chapter 7.4.2 “Fracture measurement with pictures”, although this was not studied “live” from the side as in the previous measurement. With the Craig-design there is no significant increase in the force before fracture as it was with the SW412 structure. This is because the stylus and the mass of this structure are never in parallel before fracture.

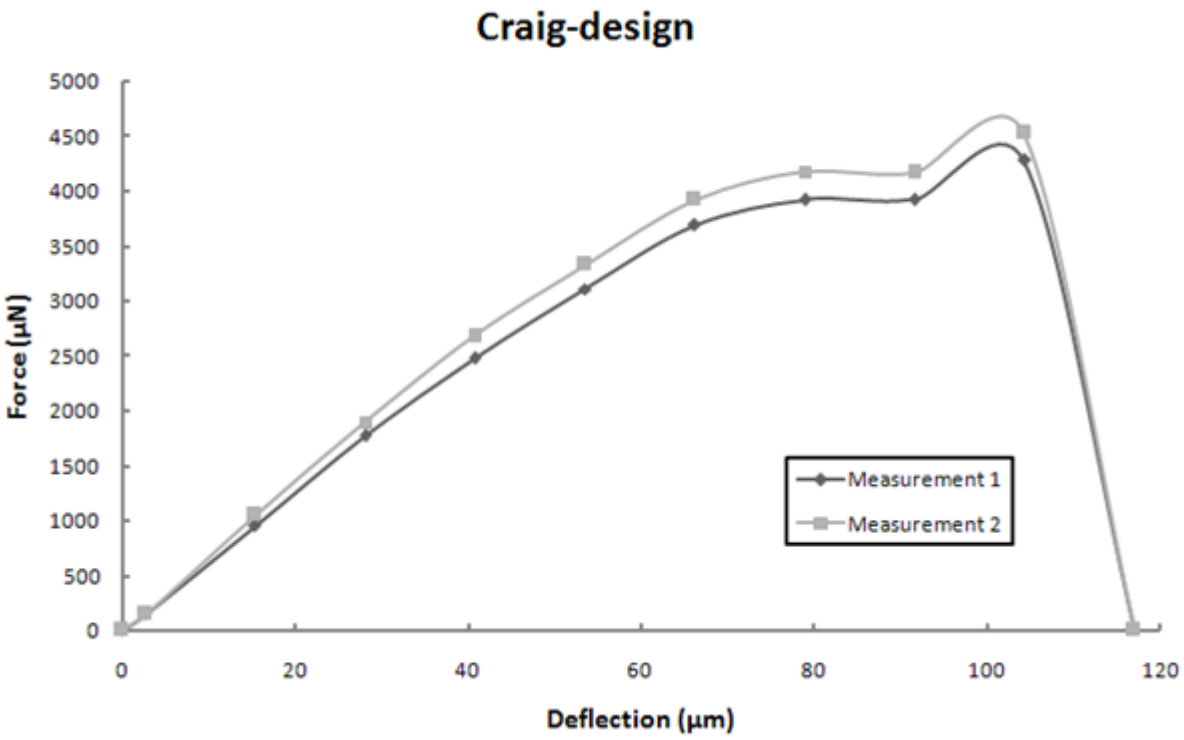

Figure 7-27: Force/deflection fracture measurement on Craig-design.

7.5 *Measurement of process variations*

For a manufacturer of MEMS-products it could be useful to have a measurement setup that could measure variations on the microstructures over a wafer, or from batch to batch. This way the manufacturer could monitor the properties of the finished products from the production line and analyze the variations to optimize the production. Since production variations from batch to batch are very small, and variations across a wafer are even smaller, such a measurement system must be very accurate. To test the force/deflection-measurement system I have done a measurement on one of the provided wafers with SW412 structures. Figure 7-28 shows measurements done on the centre of mass of six different structures on a wafer. It is the same measurement series as Figure 7-11. Three of the measurements, the blacks A2-A4, are done on structures on one side of the wafer, and the reds, M1-M3, are done on the other side of the wafer. The variation across the wafer would be expected to be bigger when the measurement is performed with the maximum distance between the measured structures.

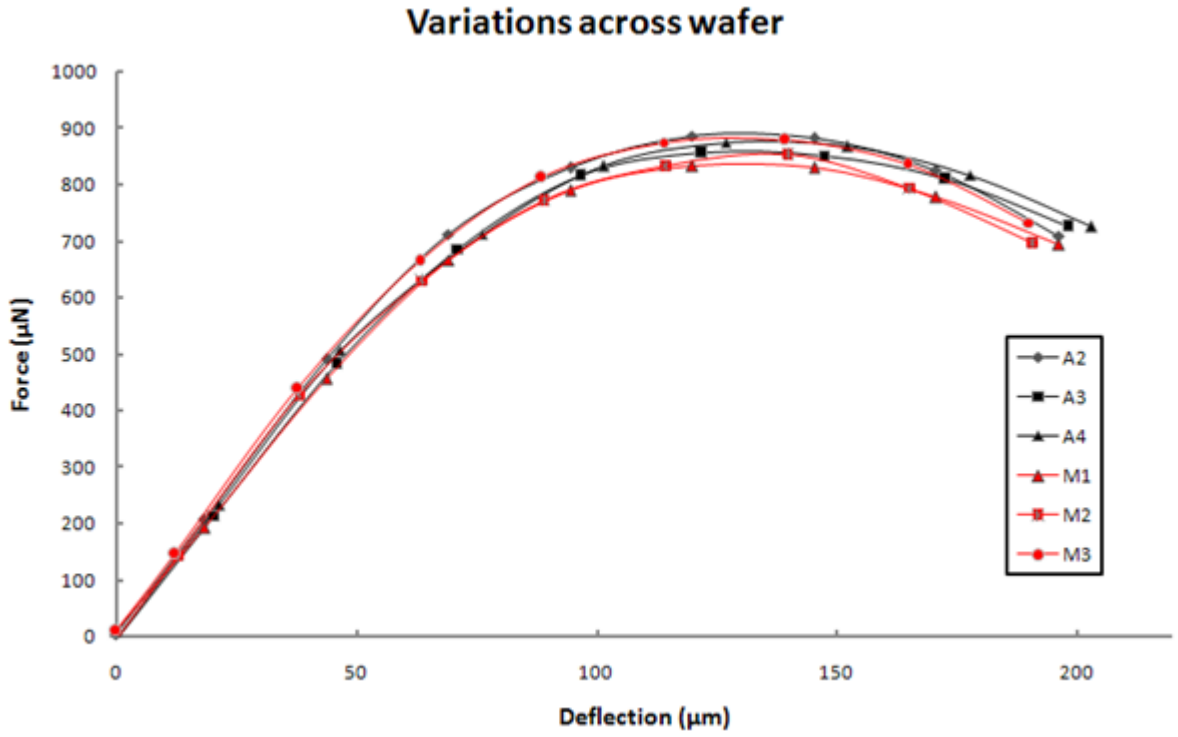

Figure 7-28: Variations across wafer.

As seen in Figure 7-28 there are some variations between the six measurements. Question is if this is measurement variations or structural variations on the wafer.

From Chapter 6.1 “Signal from loadcell” where the measurement setup was characterized the standard deviation of one point in a measurement was found to be 6.8 µN.

In addition the accuracy of the placement of the stylus was discussed in Chapter 7.1 “Stylus placement accuracy simply supported mass”. It was stated that with an error of placement in the x-direction the spring constant in the linear regime of the curve would deviate 0.1 N/m for each µm placement error of the curve. A placement error in the x-direction will also affect the shape of the curve after the linear regime. It is difficult with the current measurement setup to place the stylus on the exact same place on each structure.

In Chapter 7.4.4 “Fracture tests with different loadcell position” it was discussed the difference between the curves because of the added or subtracted moment on the tip at large deflections. Because of the physical setup of the measurement system, measurements can only be performed on the edge of the wafer and approximately 3 cm towards the middle. When performing these measurements on the edge of the wafer there will therefore be a 180 degree change in the position of the stylus relative to the structures, hence the difference in moment discussed in Chapter 7.4.4.

All of these factors give variations in the measurements done with this force/deflection measurement setup, with the error in placement of the stylus probably influencing the most. The variations in Figure 7-28 seems to coincide well with the mentioned factors. So for this measurement I conclude that the variations seen are the measurement variations. The structural variations across the wafer are simply too small to detect with this measurement setup with these measurement variations.

With the possibility to place the stylus more accurately the main reason for the measurement variations would disappear. This could be done with a more precise x-y-table. If the wafers could be aligned correctly with the x-y-table the stylus could be placed on the same place on the structures if the distances between the structures on the layout are known. Another possibility is to use a better optical instrument than the microscope used to place the stylus. By determining a reference point on the structures and placing the stylus with a more precise optical tool, much better placement accuracy could be obtained.

7.6 Measurements of bridge signals

So far all the measurements on the structures have been strictly mechanical. On MEMS-devices there are electrical contacts to readout the behavior of the structure. It would be interesting to study these electrical signals while performing a force/deflection-measurement. To accomplish this, the provided wafer with the SW412 accelerometer structures was diced in to 3x3 mm chips. Some of these chips were glued to a substrate with printed conducting lines on them so that the signals from the chip could be measured. To get contact between the chip and the conducting lines on the substrate, wirebonding was used. A probing setup was made to get the signals from the substrate, through wires, to the AD-converter. A simple Labview-program similar to the one explained in Chapter 4.3 “Software” were made to measure the electrical signals from the chip.

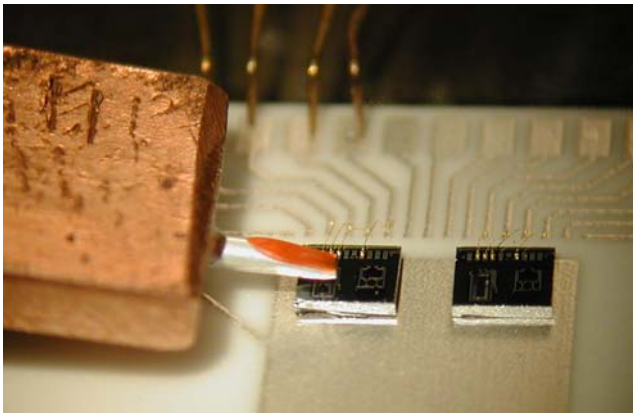

Figure 7-29: Setup for measurement of bridge signals.

Figure 7-29 shows two chips glued to a substrate. The conducting lines on the substrate and the wirebonds are also shown. In the top of the picture the four probes are in contact with the pads on the substrate. The picture was taken during a measurement, so the red and silver colored tip is the stylus of the force/deflection measurement setup.

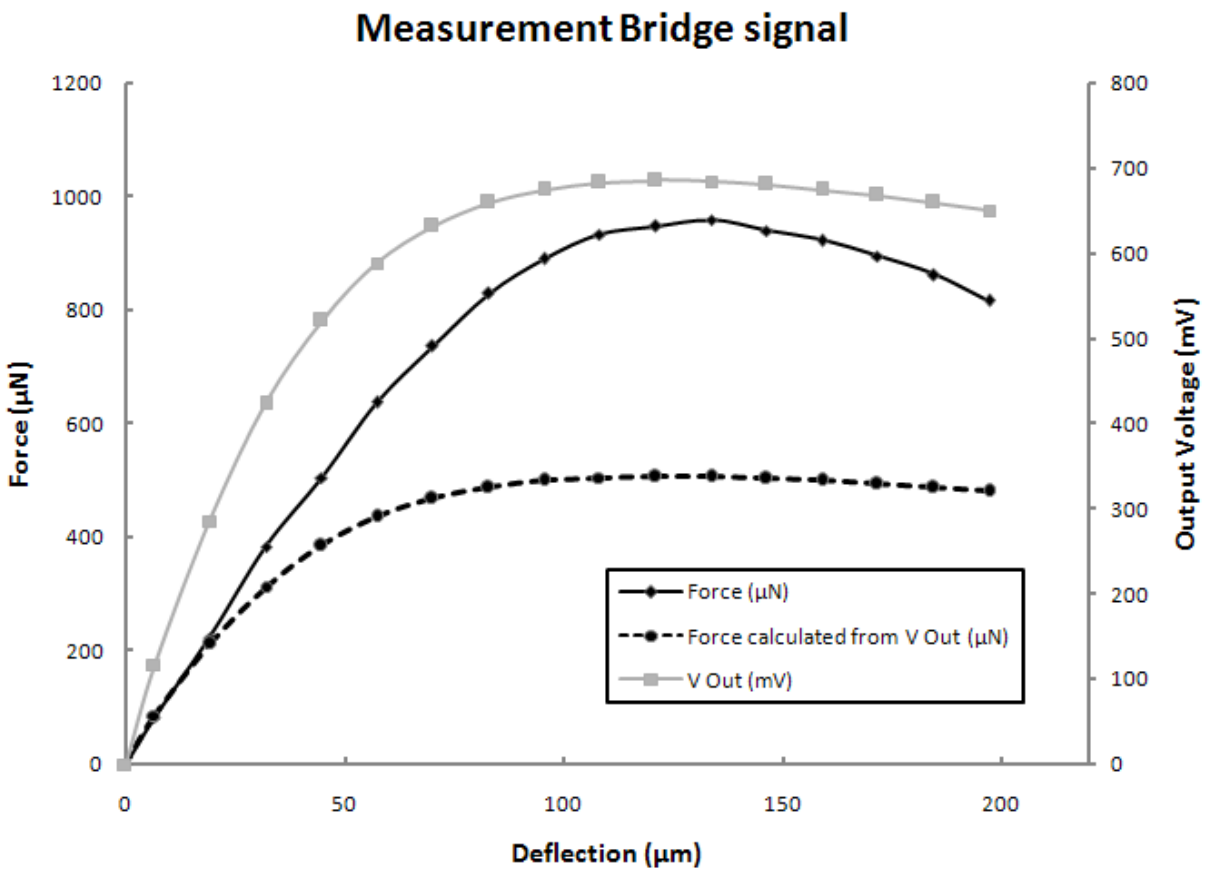

Figure 7-30: Force/deflection measurement with measurement of bridge signals.

In Figure 7-30 a force/deflection measurement with the bridge signals is shown. The black curve is a force/deflection measurement with values on the left axis. The grey curve is the bridge signal from the chip with values on the right axis. The dashed black curve is the calculated force from the bridge signal, based on the nominal value of the sensitivity (35 µV/Vg) from the datasheet of the SW412 [1]. Values of the dashed black curve are on the left axis. As seen in the figure the calculated value of the force follows the measured with small deflections and forces. In the datasheet the range of use of the SW412 sensor is set to 3000g, this is equal to 194 µN with the size of the structures mass. In Figure 7-30 it is evident that it is approximately in this area the calculated and measured force coincides. The sensitivity given in the datasheet is only valid for the beginning and relatively linear area of the curve. At larger deflections geometrical nonlinearities come in to play and the measured and V Out signal calculated force curves will deviate.

The electrical configuration on the chip is a wheatstone bridge, which for this measurement was driven by a voltage of 2.5 V. Similarly with the previously discussed behavior of the force/deflection measurement curve (discussed in Chapter 7.2 “Analysis of force/deflection curve shape”) we also see that the output voltage from the bridge flattens out and then decreases as the deflection increases. This is somewhat unexpected since as the deflection increases, the stress in the area where the resistors of

the bridge is placed will also increase. When the stress increases the output from the bridge should also increase. This is assumed all the resistors are placed in the max-stress area, they experience the same stress, and that the transversal and longitudinal resistors have the same change but with opposite signs. Since the resistors have a certain size these assumptions are not valid. In addition, as the deflection increases, the x-force explained in Figure 7-5 will come more in to play, and this will have an effect on the stress in the region of the bridge. All these conditions influence on the shape of the output voltage curve, however it was not studied further in this thesis.

From the force/deflection and V Out measurements in Figure 7-30 the sensitivity of the accelerometer can be found. To get this sensitivity with the same denomination as given in the datasheet for the sensor, the force measured in µN must be converted to acceleration in g. To do this conversion the weight of the mass of the accelerometer must be found. This is done by multiplying the length, width and height of the mass with the weight of silicon (2330 kg/m^3). The length and width given in the datasheet for the accelerometer does not reflect the N-well profile at the edge of the mass, so by measuring through a microscope more accurate values are obtained (Figure 7-31).

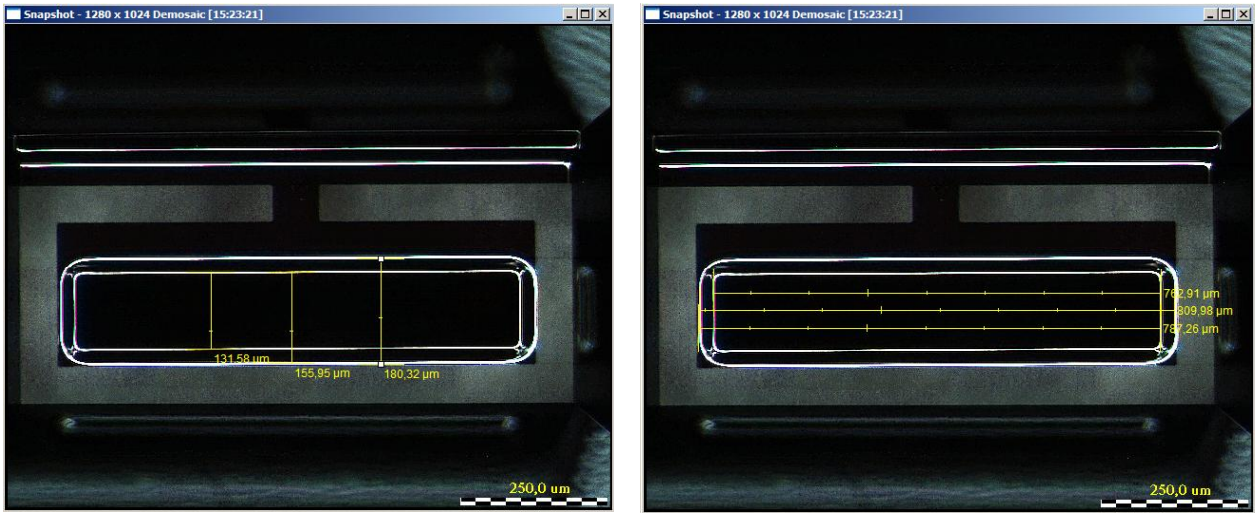

Figure 7-31: Dimensions of mass on accelerometer SW412.

By using these lengths and widths (156 µm x 787 µm) and the height given in the datasheet (23.1 µm) the weight of the mass is calculated to m=6.61*10^{-9} kg. Then the force in Newton is divided by m*9.8 to get the acceleration in g. At deflections of 6.7 µm in Figure 7-30 the force is found to be 82.9 µN and the output voltage is 117.1 mV. A force of 82.9 µN is then the same as an acceleration of the mass of 1280 g. To find the sensitivity of the accelerometer the output voltage must be divided with the drive voltage of the bridge (2.5 V) and the acceleration in g. An output voltage of 117.1 mV then gives a sensitivity of 36.6 µV/Vg. This is inside the tolerance of the datasheet of 35±10 µV/Vg [1].

By doing the same calculations at the 19.4 µm deflection values (224 µN and 286.1 mV) the sensitivity is 33.1 µV/Vg. This shows that the output voltage is not linear in this area. However this area is larger than the 3000g recommended for use in the datasheet [1]. 3000g is equal to a force of 194 µN. This is only the very beginning of the curve shown in Figure 7-30, so it is expected a certain nonlinearity when this area is exceeded.

8 Suggestions further studies

In Chapter 7 “Measurements on provided structures with analysis” force/deflection measurements on a simply supported mass accelerometer structure were analyzed. For other types of structures similar analysis needs to be performed to understand the measurements. The measurement system could be used to measure force/deflection response on all kinds of deflectable structures. If a doubly supported mass or cantilever, or a membrane, or some other structure were to be tested, a different force/deflection response would be expected and would be needed to analyzed.

The biggest source of error in the measurement system is the stylus placement accuracy. If this could be improved the measurement system would be more precise and the process variations commented in Chapter 7.5 “Measurement of process variations” might be possible to measure. This could maybe be acquired with a better X-Y-table and microscope setup, or another kind of optical instrument to align the structures and the stylus.

Trond Inge Westgaard also suggested another use of the measurements system. If the temperature on the wafer during measurements could somehow be controlled the temperature dependency of the structures could be measured. Such a temperature controlled measurement should also be combined with measurement of the bridge signals similar to the measurements done in Chapter 7.6 “Measurement of bridge signals”.

From Chapter 6.5 “Specifications vs. requirements” the wanted requirements of the measurement system was compared with the specifications of the system. The only requirement not redeemed was the diameter of the stylus tip. Because of the geometry of the stylus and the big slope of the mass of the structures at fracture it was also not possible to perform fracture tests on the SW412 structures. The possibility of using another stylus could be studied further. The question will then be if a stylus with another geometry, tip diameter or material would withstand the forces in the measurement.

9 Conclusions

A measurement system to measure force/deflection on microstructures has been built. Starting with finding the requirements for such a setup, a suitable method and parts to build it. Continuing with characterization of the measurement system, and performing force/deflection measurements on some provided structures.

The stylus measurement system built can deflect structures up to 28 mm with a resolution of 0.1 µm. This deflection has a repeatable error of 1 µm, caused by a microstep error in the Z-actuator. This could however be cancelled out with correct deflection steps. The resulting force from the deflections is measured by a loadcell. The force range of the measurement system is 0-250 µN, with a standard deviation of 6.8 µN for each force measurement. The force and deflection is measured and applied to the microstructures through a stylus with tip diameter 35.5 µm.

The measurement system was tested on some provided SW412 accelerometer structures. This is a simply supported mass accelerometer structure, and the force/deflection measurements were analyzed for this structure. The force/deflection curve from the measurements shows a nonlinear behavior. The main reasons for the nonlinear behavior of the force/deflection curve were studied “live” during measurements from a side view microscope. The two main reasons is that the measured z-force is not the same as force perpendicular to the mass as it deflects, and that the stylus slides off the centre of mass as it deflects.

Fracture tests could not be performed on the SW412 structures. This was because of the geometry of the stylus and the extreme large deflections on these structures before fracture. The mass of the structures are actually in parallel with the slope of the stylus before fracture. However fracture tests have been performed more successfully on another structure. This structure was stiffer than the SW412 structure, so the mass was never in parallel with the slope of the stylus before fracture.

The spring constant along the mass of the SW412 structures have been found with both analytical methods (calculation and simulation) and by measurements. The results from the analytical methods and the measurements coincide well.

The biggest source of error in the force/deflection measurement is the placement of the stylus on the structure. To best represent gravitational forces on the accelerometer mass the stylus should be placed on the centre of mass. With only the help of a microscope and an X-Y-table placement on the exact centre of mass can be difficult to obtain. With different size of structures and maybe reference points which can be used, the stylus placement accuracy will depend on the geometry of the structure tested.

The force/deflection measurements have also been performed together with measurement of the bridge signal on the SW412. From this the sensitivity of the accelerometer structure has been found. The sensitivity found from the measurements is within the tolerance of the sensitivity given in the SW412 datasheet [1].

10 Acknowledgements

I would like to give thanks to some people for helping me along the way in this project. First of all I am grateful to the help from my two supervisors Einar Halvorsen and Xuyuan Chen. They have been of great help during the whole project and have assisted in forming the end result. Through their expertise and help they have assured the quality in this project.

Thanks also to Trond Inge Westgaard at Infinion SensoNor Technologies who suggested this interesting project. Through occasional meetings and mails the progress and the results of the project has been discussed. He has also been very helpful in lending equipment used in this project.

Thanks to Lars Hoff for help with problems in LabView. Three of the lab engineers in VUC have also been very helpful. Thanks to Jan Erik Horntvedt for helping me with the ordering of equipment and for lending a hand in the cleanroom. Thanks to Finn M. Reinhardtsen for all the help in the mechanical workshop. And last but not least thanks to Tormod Vinsand for providing camera and for helping in the microscope lab.

11 References

[1] I. T. SensoNor, "Intern Brikke Spesifikasjon Sensorbrikke SW412."

[2] S. M. Hu, "Critical Stress in Silicon Brittle-Fracture, and Effect of Ion-Implantation and Other Surface Treatments," *Journal of Applied Physics*, vol. 53, pp. 3576-3580, 1982.

[3] S. Johansson, J. A. Schweitz, L. Tenerz, and J. Tiren, "Fracture Testing of Silicon Microelements Insitu in a Scanning Electron-Microscope," *Journal of Applied Physics*, vol. 63, pp. 4799-4803, 1988.

[4] C. J. Wilson and P. A. Beck, "Fracture testing of bulk silicon microcantilever beams subjected to a side load," *Journal of Microelectromechanical Systems*, vol. 5, pp. 142-150, 1996.

[5] A. C. Ugural and S. K. Fenster, *Advanced strengt and applied elasticity*, Fourth edition ed: Prentice Hall, 2003.

[6] http://www.matweb.com/index.asp?ckck=1.

[7] O. Kraft and C. A. Volkert, "Mechanical testing of thin films and small structures," *Advanced Engineering Materials*, vol. 3, pp. 99-110, 2001.

[8] G. M. Pharr and O. W. C., "Measurement of thin film mechanical properties using nanoindentation," *MRS Bulletin*, vol. 17, pp. 28-33, 1992.

[9] M. W. Denhoff, "A measurement of Young's modulus and residual stress in MEMS bridges using a surface profiler," *Journal of Micromechanics and Microengineering*, vol. 13, pp. 686-692, 2003.

[10] M. Hopcroft, T. Kramer, G. Kim, K. Takashima, Y. Higo, D. Moore, and J. Brugger, "Micromechanical testing of SU-8 cantilevers," *Fatigue & Fracture of Engineering Materials & Structures*, vol. 28, pp. 735-742, 2005.

[11] X. G. Xiong, Q. Zou, D. Lu, and W. Y. Wang, "Balance-approach for load-displacement measurement of microstructures," *Mechatronics*, vol. 8, pp. 549-559, 1998.

[12] Y. Higo, K. Takashima, M. Shimojo, and S. Sugiura, "Fatigue testing machine of micro-sized specimens for Mems applications," *Materials research society symposium*, vol. 605, pp. 241-246, 2000.

[13] E. Peiner and L. Doering, "Force calibration of stylus instruments using silicon microcantilevers," *Sensors and Actuators a-Physical*, vol. 123-24, pp. 137-145, 2005.

[14] S. Cao, U. Brand, T. Kleine-Besten, W. Hoffmann, H. Schwenke, S. Butefisch, and S. Buttgenbach, "Recent developments in dimensional metrology for microsystem components," *Microsystem Technologies*, vol. 8, pp. 3-6, 2002.

[15] C. Lowrie, C. Grinde, L. Hoff, and M. Desmulliez, "Piezoresistive Three-Axis Accelerometer for Monitoring Heart Wall Motion," presented at Proceedings of the Symposium on Design, Test, Integration and Packaging of MEMS/MOEMS, Montreux, Switzerland, 2005.